Particle Formation and Models in Internal Combustion Engines

David Kittelson[1] Markus Kraft[2]

released: 31 January 2014

[1] Department of Mechanical Engineering
University of Minnesota
111 Church St. SE
Mechanical Engineering
MN 55455
USA
E-mail: kitte001@umn.edu

[2] Department of Chemical Engineering
and Biotechnology
University of Cambridge
New Museums Site
Pembroke Street
Cambridge, CB2 3RA
United Kingdom
E-mail: mk306@cam.ac.uk

UNIVERSITY OF
CAMBRIDGE

Abstract

This article reviews work on aerosols originating from internal combustion engines with an emphasis on soot formation during in-cylinder combustion. Mathematical models of particle formation in engines and remaining modeling challenges are also discussed. Aerosols are formed during combustion in the cylinder, in the exhaust system and after the tailpipe. Specific mechanisms include the injection of fuel, formation and oxidation of particles during combustion, exhaust gas recirculation (EGR) and condensation of semi-volatiles. The role of fuels is discussed with respect to their ignition behavior as a consequence of mixture preparation in the cylinder and with respect to their sooting propensity. Models for the formation, growth and oxidation of soot particles are presented and the most popular mathematical approaches for simulating particle emissions are introduced. Solid and semi-volatile nucleation mode particles are also discussed in some detail. Key drivers in the formation of these particles are lubricating oil metals and sulfur in the fuel and oil. Particle emissions of different types of gasoline engines with and without aftertreatment are also mentioned and compared with diesel engine emissions. Some of the short comings of the current models and future research areas are highlighted at the end.

Contents

1 Introduction

Aerosols form in almost any type of internal combustion engine (Kittelson [44]; Eastwood [17]) and have been identified as a potential health risk (Stone and Donaldson [78]). In particular exhaust from older technology diesel engines was shown to be human carcinogen (Benbrahim-Tallaa et al. [8]). Legislators around the world have reacted to the adverse health effects of particles by introducing an ever more stringent set of regulations; see for example REGULATION (EC) No 715/2007 for *compression ignition* (diesel) and *positive ignition* (gasoline, NG, LPG, ethanol, etc.) vehicles. There is now considerable pressure on original equipment manufacturers (OEMs) and suppliers to develop engines that are able to meet these more stringent standards while minimizing cost and fuel economy penalties. The present approach to meeting these standards with diesel engines generally involves the use of diesel particulate filters which reduce exhaust particle matter (PM) to very low levels. But even when filters are used it is necessary to reduce engine out particulate matter to the lowest practical level in order to avoid fuel consumption penalties associated with excessive backpressure and frequent regeneration. In order to be able to do this it is necessary to understand what processes cause the formation of particles during engine operation and what role fuels play. In the last decade, considerable progress has been achieved using better injection and air handling systems and better engine control. The increasing use of biomass derived fuels like biodiesel (fatty acid methyl ester or FAME) adds another dimension to the problem.

Engine aerosols are more complex than those formed in laboratory flame studies because the intermittent nature of engine combustion, complex flow patterns and wall interactions, and the presence of lubricating oil which contributes organic carbon (OC) and metal compounds to the exhaust aerosols. The presence of sulfur in the fuel and lubricating oil is a further complication. Sulfur is not present at sufficiently high levels to influence the main combustion processes but it influences the formation of the exhaust aerosol as it cools and dilutes in the atmosphere. The roles of lubricating oil and sulfur compounds will be considered separately from soot formation.

The purpose of this article is to provide an overview of how aerosols form in engines and what happens to them as they dilute and cool in the atmosphere. The nature of aerosols is described and specific mechanisms of their formation are discussed. These mechanisms include injection of fuel, combustion, the formation and oxidation of particles. The role of fuels will be discussed with respect to their ignition behavior and with respect to their sooting propensity. Formation, growth and oxidation of carbonaceous particles will be studied in more detail and the most important mathematical modeling approaches will be introduced. Finally, particles that are not formed by the primary combustion process are considered. These include ash particles and semi-volatile particles formed from partially burned lubricating oil and fuel and sulfur compounds. Particle emissions of different types of gasoline engines with and without aftertreatment will be also mentioned and compared with diesel engine emissions. Some of the current short comings and future needs will be highlighted at the end.

2 Aerosols in Engines

2.1 What are aerosols from engines made of and where do they form?

Whitby and Cantrell [87] were the first to identify three different modes observed in engine aerosols. These modes are comprised of a "nucleation mode", an "accumulation mode" and a "coarse mode" all displayed in Fig. 1. The nucleation mode consists of aerosols of diameters ranging between about 3 to 30 nm composed mainly of volatile organic and sulfur compounds that form as exhaust dilutes and cools. It typically contains less than 10% of the particle mass but more than 90% of the particle number. The accumulation mode ranges from about 20 to 500 nm and consists mainly of carbonaceous agglomerates and adsorbed material. This mode contains most of the particle mass. The coarse mode, typically 5-20% of particle mass, consists of accumulation mode particles, which deposited on the surfaces of the cylinder and exhaust system and re-entrained at a later stage, and atomized lubricating oil from the crankcase. The size ranges and boundaries of the modes may shift and overlap with changes in engine, fuel, and operating conditions, but the fundamental structure remains. The distinction between the modes is not size but formation mechanism. Even aircraft gas turbine engines exhibit a similar modal structure in the submicron region, although the particle diameters are typically smaller than for diesel or spark ignition engines. It is important to note that the transition between the modes, the modal diameter and concentration may vary based on dilution and sampling condition as sulfur and organic compounds are generally in the vapor phase in the tailpipe and only undergo the gas-to-particle formation as the exhaust is diluted and cooled. Figure 1 also shows some standard definitions of atmospheric particles: PM10, fine particles, ultra-fine particles and nanoparticles for comparison. TEM images of particles originating from the submicron modes are displayed in Fig. 2: carbonaceous agglomerates that contribute most of the mass in the accumulation mode, semi-volatile droplets that usually comprise most of the number in the nucleation mode, and tiny ash particles that may either decorate existing particles as shown or form separate solid particles in the nucleation mode size range (Jung et al. [35]).

Figure 3 shows the processes responsible for the formation of particles during combustion, dilution and cooling. These conditions are representative of a heavy duty diesel engine under typical cruise conditions. In an early stage carbonaceous particles are formed during combustion and most of them are oxidized. In addition lubricating oil is entrained into burning fuel jets and may also form carbonaceous particles as combustion products. There is also evidence that metallic additives in the lube oil such as Ca and Zn may be converted to gas-phase compounds, and then undergo gas-to-particle conversion as products of combustion expand and cool. Most of the resulting particles end up decorating accumulation mode particles, but separate ash nucleation may form when the ratio of ash to carbonaceous accumulation mode particles is sufficiently high (Abdul-Khalek et al. [3]; Jung et al. [35]; Lee et al. [53]). Upon exit from the tailpipe, dilution and cooling leads to gas to particle conversion of semi-volatile materials, mainly hydrocarbons (in the volatility range of lubricating oil) and sulfuric acid leading to homogeneous and heterogeneous nucleation and adsorption/condensation on existing particles (Tobias et al. [82]; Ziemann et al. [91]; and Sakurai et al. [68],[69]). During dilution and cooling there is a
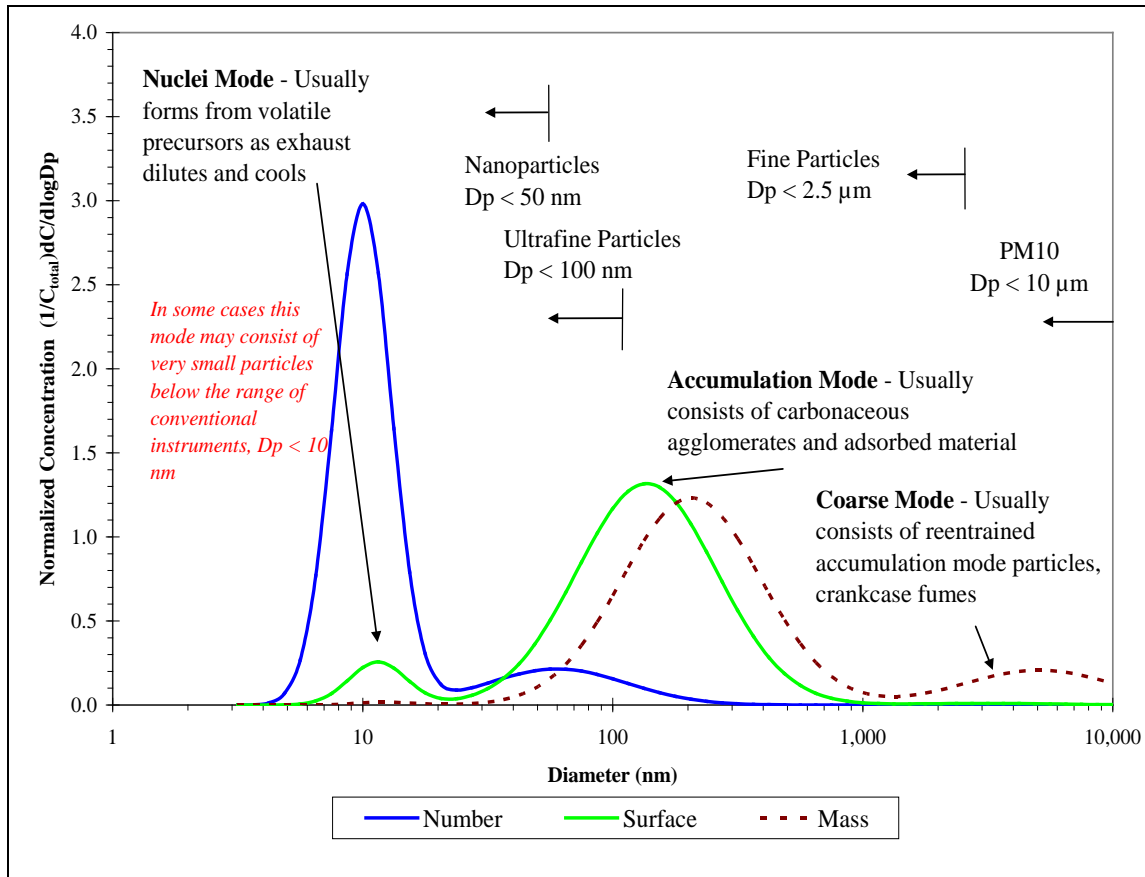
Figure 1: *Typical engine exhaust particle size distribution by mass, number, and surface area. Dp is the aerosol particle diameter (adapted from Kittelson [44]).*

competition between nucleation and adsorption onto existing particles. Fast dilution and low concentrations of accumulation mode soot particles relative to materials undergoing gas to particle conversion favor nucleation over adsorption onto existing particles. Under light load and idle condition the temperature in the exhaust system may be low enough for nucleation of volatiles to occur there (Kittelson et al. [47]).

The processes in Fig. 3 will now be considered in greater detail. The first steps of particle formation shown highlighted in the bold oval, *i.e.* the formation of carbonaceous particles and their oxidation will be considered first. Then the fate of these particles and semi-volatile particle precursors as the exhaust dilutes and cools in the atmosphere will be described in more detail.

2.2 Fuel injection, combustion and soot formation

In both compression ignition engines as well as in direct injection spark ignition engines, fuel is injected into the cylinder in form of a spray. The interaction of the spray with the in-cylinder gases is very complex and influences the local composition of gases which in
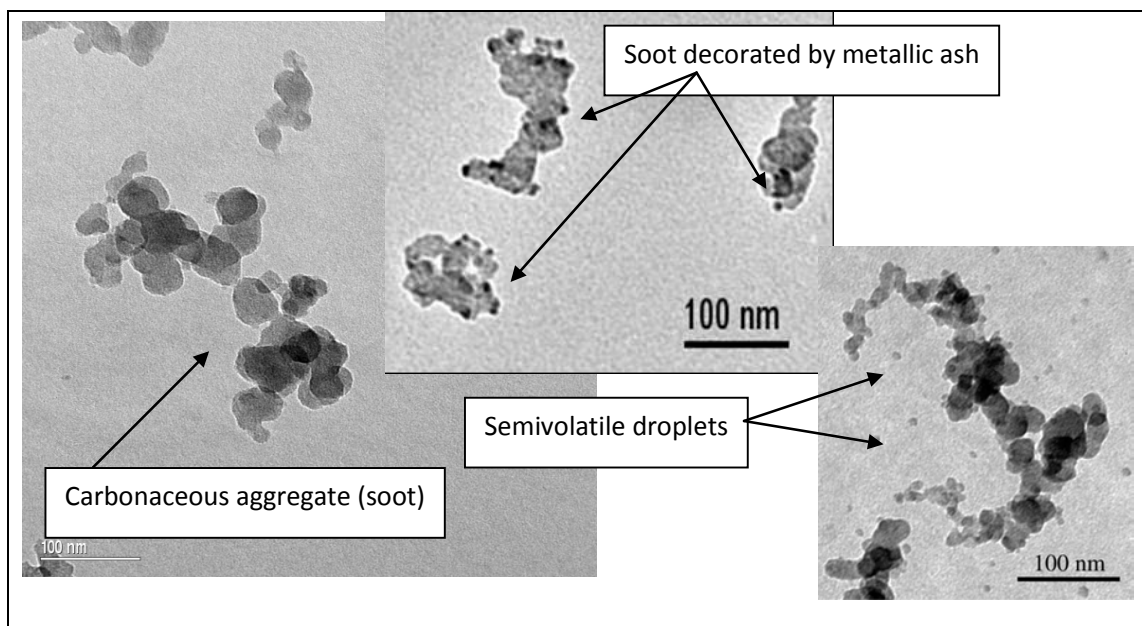
5

Figure 2: *Engine exhaust particles are very diverse in size, shape, and composition (adapted from Jung et al. [35] and Miller et al. [61]).*

turn influence the formation of particles and other combustion products. The liquid fuel jet often exceeds the thermodynamic critical point of the liquid and at present there exist no first-principles model which is able to describe this mixing process. The break-up of the jet, local gas mixture composition and wall impingement have strong influence on engine performance and engine emissions.

Although there is no first-principles quantitative model available, optically accessible engines have provided some insight into this complex process of injection of the fluid, spray formation and the resulting combustion followed by soot formation. The seminal paper by Dec [16] and further publications by the Sandia group, *e.g.* (Flynn et al. [19]) have put forward a conceptual model of the processes occurring in the cylinder shortly after injection of the fuel (See Auto120 for more details).

Following this model the physical and chemical processes taking place in a fully developed burning plume in the cylinder of a diesel engine is shown in Fig. 4. A cold fuel jet and entrained hot air enters a diffusion flame sheath at a local temperature of around 825 K. As the fuel/air mixture travels through the plume it reacts under rich premixed conditions to form products of rich combustion, for example CO and species that can be classified as unburnt hydrocarbons (UHC) but in particular acetylene and probagyl radicals. At temperatures higher than 1300 K latter species triggering fast polymerization reactions leading to polycyclic aromatic hydrocarbons (PAHs) that are considered to be the building blocks for particulates in flames. As these small particles travel down the plume they grow in mass through condensation of PAHs, further polymerization reactions and agglomeration to form particles of the size and shape emitted from an engine's
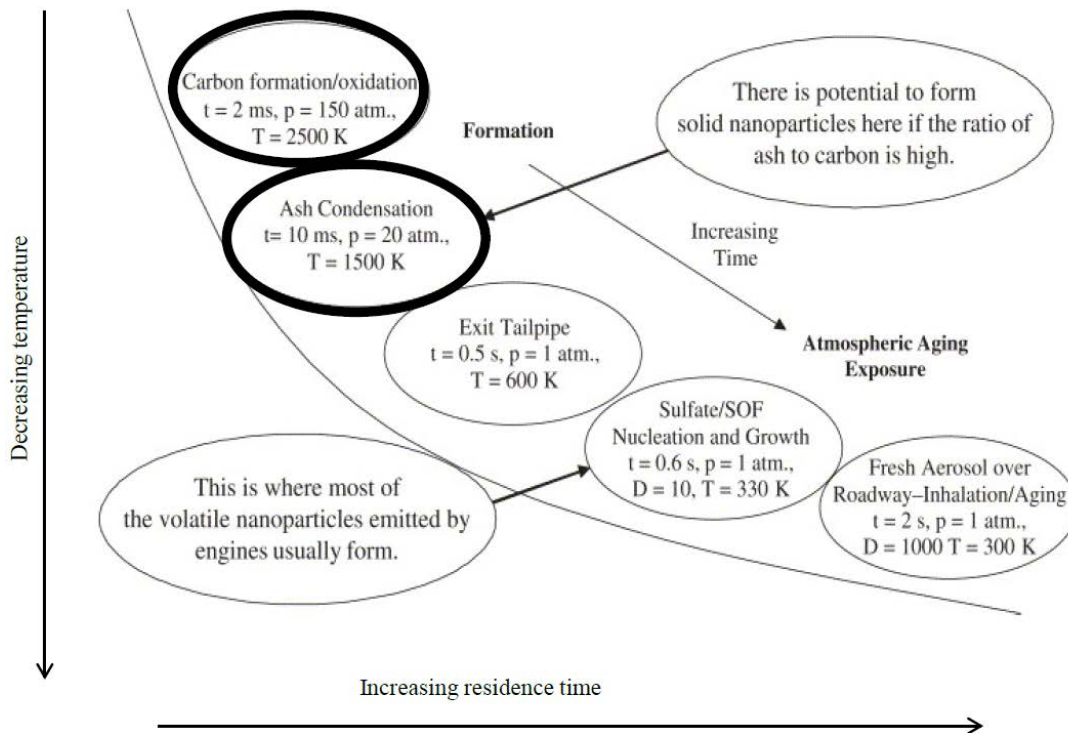
6

Figure 3: *History of particle formation in a compression ignition engine (adapted from Kittelson et al. [47]).*

tailpipe. However, as these particles and UHC pass through the very thin diffusion flame sheath fuel fragments and particles are converted to CO_2 and water vapor during rapid heat release. As a consequence the temperature in this region is high and can lead to considerable NO_x formation. Diesel soot particles are the result of quenching this final phase of oxidation.

The time evolution of the plume was also studied using an empirical combustion and soot model implemented into a CFD code by Kazakov and Foster [39]. Figure 5 shows a simulation of the time evolution of temperature and soot formation during the injection of the fuel. After ignition, the flame forms a three dimensional plume-like structure which comprises different kinds of combustion modes. The flame propagating along the outermost region of the plume reaches, the tip of the liquid spray, and then reaches the tip of the plume. The highest temperatures are found along the stem and the border of the cup like structure. Inside the stem there is a zone of intensive droplet evaporation. Although this model is unable to predict the existence of a premixed combustion zone inside the stem due to the simplified chemical model, the initial location of the soot cloud and its temporal evolution are in qualitative agreement with the schematics introduced by the Sandia group ([19]). This soot cloud will then impinge on the bowl wall and follow around the
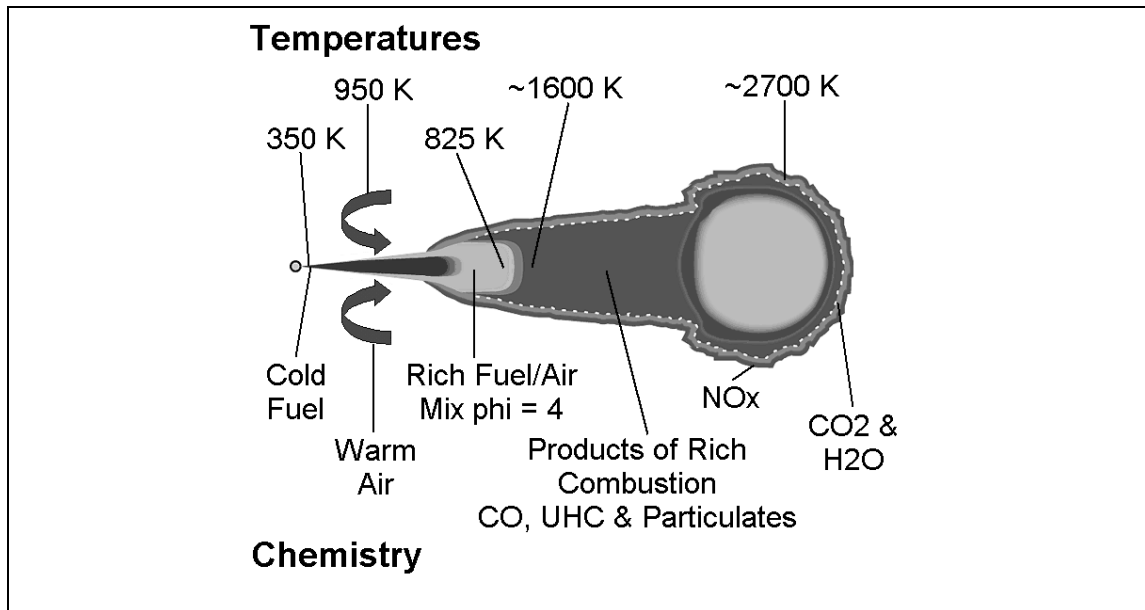
Figure 4: *Structure of the sooting plume after injection and ignition (adapted from Flynn et al. [19]).*

cylinder boundaries while undergoing continuous oxidation. Soot travelling to the low temperature regions close to the cylinder walls will not be oxidized and will remain as a combustion product in the exhaust.

2.3   The role of exhaust gas recirculation (EGR)

Many engines recirculate part of the exhaust to modify charge composition and temperature aiming to reduce emissions in general and NO_x emissions in particular. Exhaust gas recirculation (EGR) can also have a significant effect on the particle size distribution. Although most of the particles in the EGR that re-enter the cylinder will be oxidized and transformed into CO_2 some of the particles may survive and can grow substantially. The mechanism by which this happens has been studied in an SI engine converted for single-cylinder HCCI operation (Mosbach et al. [62]) using *n*-heptane as fuel, at an equivalence ratio of $\varphi = 1.93$. Particle-laden in-cylinder gases were extracted through snatch sampling, accumulated over a number of cycles in steady-state operation. The captured aggregates were analyzed through a Scanning Mobility Particle Sizer (SMPS) and a High-Resolution Transmission Electron Microscope (HRTEM). Figure 6(a) shows the time evolution of the aggregate size distribution between 5 and 65 CAD ATDC. In a later stage of the cycle the distribution turns bimodal, since inception is present throughout and large aggregates collect the small particles. In Fig. 6(b) aggregate size distributions at 10 CAD ATDC are plotted for ten consecutive cycles. The first cycle starts without any soot present in the residual gases. Within ten cycles the distribution has stabilized and the statistical noise has decreased substantially. The consecutive growth of aggregates in each cycle can be
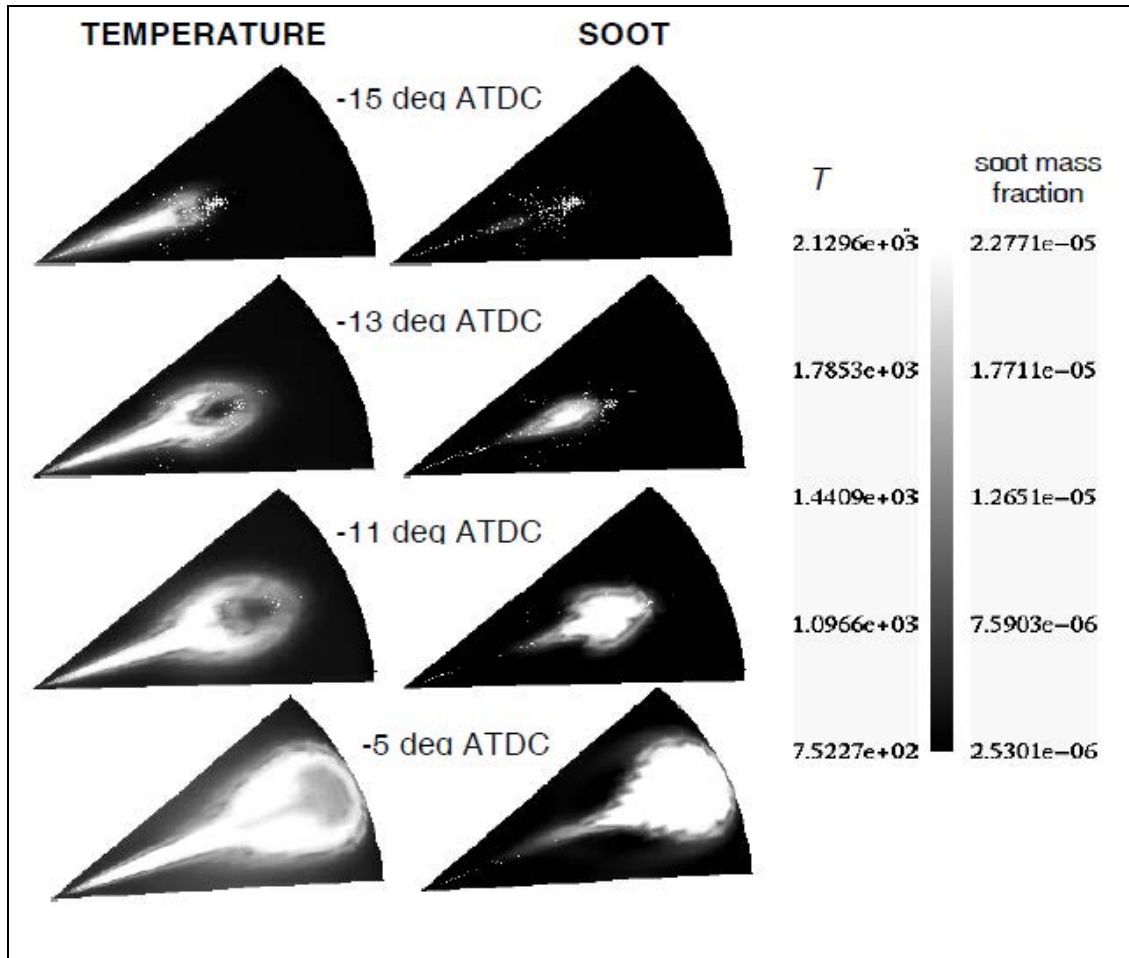
Figure 5: *Temporal sequence of temperature and soot in a fuel jet after injection (adapted from Kazakov and Foster [39]).*

clearly identified from this figure. In fact aggregates larger than about 20 nm are recirculated for possibly several times before being emitted from the engine. As mentioned above in a diesel engine most of these large aggregates will be oxidized but the surviving particles act as sponge collectors for other particles, remaining fuel droplets and engine oil. These particles often cause fouling of other engine components such as swirl flaps found in modern diesel engines.

3 Fuel Effects

3.1 Mixture preparation and ignition delay

The choice of fuel and its resistance to ignition plays an important role in the process of particle formation as it also influences the local mixture. This is demonstrated in Kalghatgi et al. [37] and Smallbone et al. [75] in a Partially-Premixed Compression Ig-

Figure 6: *(a) Time evolution of the size distribution with aggregates present in the trapped residual gases. (b) Size distribution at 10 CAD ATDC for ten consecutive cycles. The recirculated aggregates can be clearly identified as the ones larger than about 20 nm (adapted from Mosbach et al. [62]).*
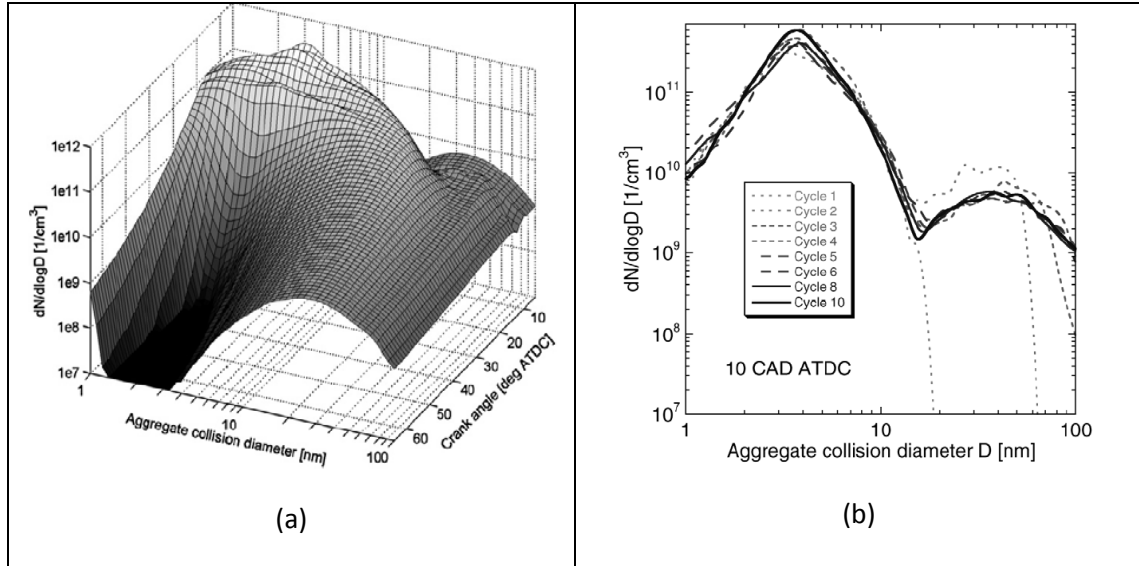
nition (PPCI) engine by increasing the resistance of fuel to ignition and observing the transition from mixing controlled to kinetically-controlled combustion. Using the srm 6.1 (Stochastic Reactor Model) engine code (srm [76]) it is shown that the difference in ignition behavior leads to different local equivalence ratios, which has a strong impact on particle formation. Figures 7(a)-(g) show the in-cylinder composition at different crank angles in an equivalence ratio-temperature diagram also called φ-T or Kamimoto diagram (Kamimoto and Bae [38]). Two different model fuels are used: *n*-heptane which was chosen as a diesel surrogate and 84 PRF as a gasoline fuel surrogate with higher resistance to ignition. Each fuel is injected in a single pulse at -8.0 CAD ATDC. Each point on the φ-T diagram represents a zone in the engine with the corresponding φ-T composition. Two regions are highlighted which are known as soot and NO_x islands. Shortly after injection the distribution of both fuels are almost identical exhibiting both lean and rich regions. Rich regions have lower temperatures due to charge evaporation. The subtle difference between the two fuels on the rich side is caused by low temperature heat release (cool flame) of *n*-heptane. This results in an earlier ignition of *n*-heptane and leads to the formation of particles as the rich zones traverse the soot island. Figure 7(h) shows the computed particle size distribution at different CADs for *n*-heptane. As the particle laden zones become leaner through mixing oxidation reduces the total number of soot particles over time. The gasoline-like 84 PRF fuel ignites later in the cycle allowing more time for mixing and ignition occurs at a lower equivalence ratio in both the lean and rich directions. As the overall mixture is burnt at leaner conditions, regimes associated with excessive PM formation are avoided. However, both fuels lead to significant NO_x emissions.

(a) -4 CAD aTDC

(b) -2 CAD aTDC

(c) -1.4 CAD aTDC

(d) TDC
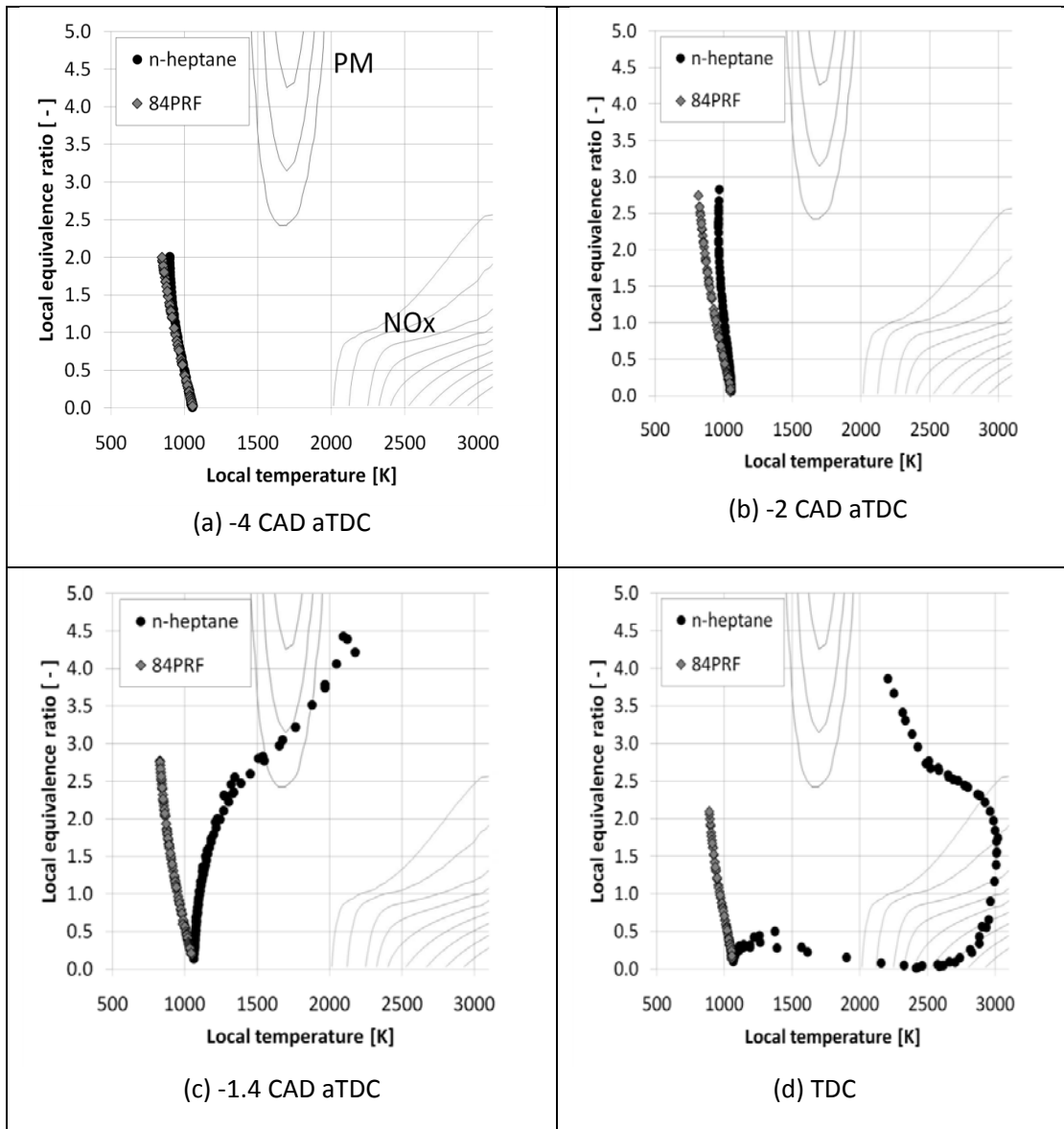
3.2 Sooting propensity practical fuels

So far reference fuel models have been designed to mimic ignition behavior which has a strong influence on soot formation as this has implication on the mixing of cylinder charge as demonstrated in Smallbone et al. [75]. However, practical fuels consist of many more chemical compounds which contribute to different degrees to the formation of particle matter. This sooting propensity is tested in a standardized procedure using a smoke point lamp. The smoke point is the height of the flame at which soot can be observed with the naked eye. The first studies trying to relate the molecular structure of hydrocarbons with the smoke point were published by Hunt [30] and Schalla and McDonald [71]. The results
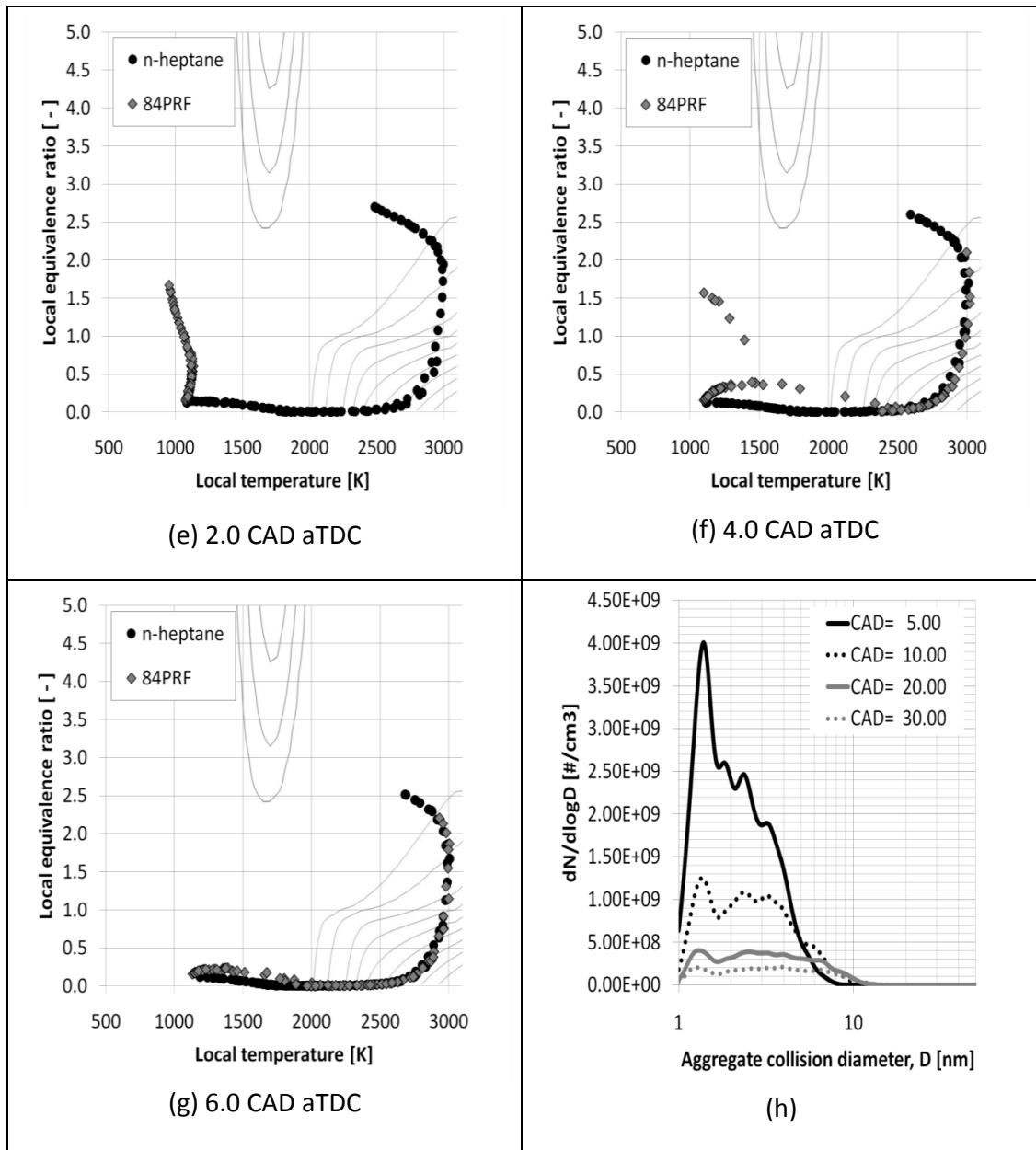
Figure 7: *In-cylinder local equivalence ratio versus temperature (adapted from Smallbone et al. [75]).*

indicated that the rate at which hydrocarbons produced soot increased as follows:

paraffins < isoparaffins < mono-olefins < naphthenes < alkynes < aromatics.

While this statement is qualitatively true, the inequality signs are not of equal weight (Calcote and Manos [11]). In general one can say the more compact the molecular structure for the same number of carbon atoms, the greater the tendency to soot. Therefore iso-

meric or cyclic alkanes and alkenes have a higher sooting propensity. However, this effect is small compared with the increase in sooting tendency if the fuel has aromatic character. The difference in sooting propensity has been explained by the difference in formation of soot precursors during pyrolysis of the fuel as the result of a dehydrogenation process of fuel molecules (Schalla and McDonald [71]). Alkylated aromatics show complex behavior as increasing the number of side chains increases the sooting tendency, whereas lengthening the chain has the opposite effect. The chances of dehydrogenation increase with the stability of the carbon structure, facilitating the removal of hydrogen atoms in comparison with the breaking of carbon bonds. The more readily the hydrogen atoms are removed as compared to the breaking of carbon bonds, the greater is the probability of smoke formation. How these findings translate to the combustion in a diesel engine is not entirely clear as the temperature and pressure histories of the air fuel mixture experienced in an engine are different to those experienced in the smoke point lamp.

4   Soot

Although experiments reveal the sooting propensity of different fuels it is far less clear how soot particles actually form, grow and oxidize. The current understanding of these processes is displayed in Fig. 8 (Sander et al. [70]).
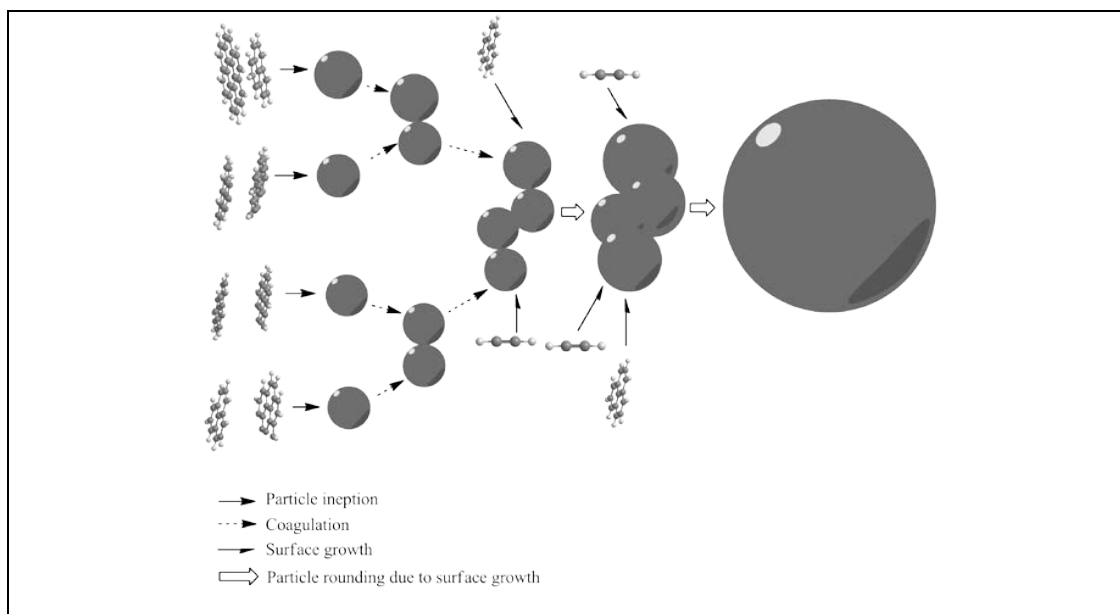

Figure 8: *Important processes in soot growth (adapted from Sander et al. [70]).*

4.1 Formation and growth

The analysis of soot particles suggest that Polycyclic Aromatic Hydrocarbon (PAH) molecules play an important role in the formation of soot as they are considered to be a key precursor molecule in the study of soot formation (Homann [29]). Pericondensed PAHs consist of six-membered rings and have been found in flames with typical temperatures ranging from 1500-2000 K as they are thermodynamically more stable than many other PAHs (Stein and Fahr [77]). Important examples of pericondensed PAHs are naphthalene ($C_{10}H_8$), pyrene ($C_{16}H_{10}$) and coronene ($C_{24}H_{12}$). The smallest PAH and building block is benzene which can form through a number of channels (Frenklach et al. [22]; Frenklach and Wang [21]). The addition of C4 species to acetylene and combination of C3 species are thought to be the most important reactions in the formation of the first aromatic ring but many other pathways exist. This PAH building block grows further by an entropy driven process of acetylene addition and hydrogen abstraction reaction called the HACA mechanism (Wang [86]). This means that although the growth of larger aromatics is slightly endothermic the abstraction of hydrogen leads to an increase in entropy and reduces the overall Gibbs free energy, which drives the growth. The transition from chemical species to a condensed phase particle is still not quite understood, however it is recognized that both physical and chemical processes play a role. The extent to which each process contributes depends on local species composition and temperature. Three pathways have been hypothesized. The first pathway assumes two-dimensional growth leading to fullerene type structures (Homann [29]). Pathway two assumes physical clustering upon collision of PAHs by dispersive forces (Frenklach and Wang [21]). Pathway three assumes that PAHs form chemical bonds after or during dimerization (Violi et al. [84]). Although pathway one exists and in low-pressure premixed flames can lead to substantial formation of fullerenes the bi-modal nature of the Particle Size Distribution Function (PSDF) requires that inception and growth process is of second order, *i.e.* two molecules forming the first particle. Since pathway three requires the presence of aryl radicals this mechanism can only be significant in the flame zone but cannot explain the formation of soot in the post flame region. Therefore most detailed soot models are based on the second pathway in which the dimerization of PAHs lead to the first soot particle. HRTEM images of small soot particles and theoretical calculation based on energy minimizations of PAH clusters support this view. Figure 9(a) shows a TEM-style projection of 50 coronene molecules assuming a low energy position (Totton et al. [83]) clearly revealing PAH stacks which can also be identified in HRTEM images of small soot particles in Fig. 9(b) (Mosbach et al. [62]).

These soot particles grow through further condensation of PAHs, continuing carbon addition by the HACA mechanism but most importantly by coagulation. In addition, photoionization aerosol mass spectrometry (PIAMS) measurements of soot in laminar premixed ethylene flames also indicate the presence of a sizable amount of aliphatic components. The presence of aliphatic components is consistent with the liquid-like nature observed by TEM and the low C/H ratio calculated from the mass spectrum (Wang [86]).

In the early phases of particle growth the PAH mobility plays an important role. PAHs of adjacent small particles are mobile and coalesce into bigger primary particles (Neer and Koylu [63]; Chen et al. [13]). This sintering process becomes less important as the size of
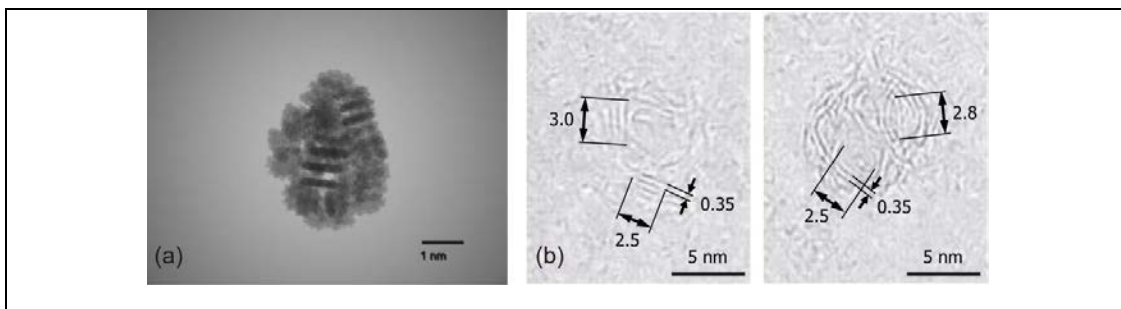
Figure 9: *(a) TEM-style projection of a cluster of 50 coronene (Totton et al. [83]) and (b) experimental HRTEM images of small soot particles sampled from an engine (Mosbach et al. [62]).*

the particles increases. Then collisions of such primary particles form aggregates, which can change their fractal dimension by further carbon addition through PAH condensation and HACA growth. The large particles act as "vacuum cleaners" and collide with many small particles, which then sinter into the larger aggregate. The collision rate at which this happens is dependent on the size of the colliding particles, local pressure and temperature. The two limiting cases are the free molecular regime (Knundsen number Kn > 10) in which particles are small enough to not constantly collide with the bath gas and the other limiting case is the continuum regime (Kn<1) in which the particles move in the bath gas as in a continuous fluid. In the high pressure - high temperature environment of an internal combustion engine most of these coagulation events take place in the continuum regime. The higher the pressure the more coagulation events take place and the larger the particles that form.

4.2   Soot oxidation

Most of the soot particles, under normal circumstances, are ultimately oxidized. Detailed oxidation mechanisms are not available as the composition of soot is not known in detail. In a review Lighty et al. [55] suggested that the reactions with molecular oxygen (O_2), oxygen radical (O), and hydroxyl radical (OH) are the main pathways of soot oxidation. The OH pathway has been identified to be predominant. From 10%-30% of collisions between a soot particle and OH radicals lead to oxidation. The rates for O_2 oxidation are derived from pyrolytic graphite. The most popular model based on graphite oxidation is Nagle-Strickland-Constable (NSC) model, which is fitted to a temperature range of 1273 K to 2673 K.

As a result of oxidation the structure of soot particles changes and can lead to fragmentation. This will lead to a substantial increase of particle number. It has been suggested that particles not only shrink but also burn from the inside hollowing particles, which eventually leads to fragmentation (Lighty et al. [55]). However, there is no quantitative understanding of these processes and some findings in the literature are contradictory and fragmentation may not occur at all. Higgins et al. [27], and Jung et al. [35], [36] studied

the oxidation of soot from flames, diesel and bio-diesel as well as the role of metals using electron microscopy and tandem differential mobility analysis (TDMA). They report that the values of activation energies for O_2 vary widely depending on temperature and origin, *i.e.* composition of soot. Diesel soot shows significantly lower activation energies compared to flame soot. Typical values for the activation energy in the O_2 reaction rate for the temperature range of 800 °C to 1000 °C is 170 KJ·mol^{-1} for flame soot and 110 KJ·mol^{-1} for diesel soot. This difference is attributed to the presence of metals in the diesel fuel, possibly coming from lubricating oils. In separate studies of Lall and Zachariah [52] in which cerium and iron was added to diesel fuel it could be demonstrated that the activation energy was found to be significantly lower than non-doped soot particles, which supports the assumption that indeed metal particles are responsible for the faster oxidation of engine derived soot. A further increase of the oxidation kinetics was observed from soot originating from bio-diesel.

5 Mathematical Models of Soot

Soot models can be characterized in terms of the type and state space they use (Kraft [49]). The type space defines how many quantities are used to represent individual soot particles, *e.g.* mass, mass and surface, or mass, detailed aggregate structure, and molecular composition. The state space tells how the entirety of particles is mathematically described. For example, the (multivariate) particle size distribution can be described in terms of its statistical moments, approximated by "sections" or by an empirical distribution as a set of discrete measures also called stochastic particles, which represent soot particles. The detail of the soot model is limited by the detail of the gas-phase chemistry model as some of the detailed soot models require an accurate knowledge of the gas-phase species that surround them.

Many simplistic models represent only the total mass of soot particles, *i.e.* soot is represented by one number. The most prominent example of such a model is the Hiroyasu (Hiroyasu and Kadota [28]) and the Hiroyasu/Nagle and Strickland-Constable (Jung and Assanis [34]) model. These models represent a mainly empirical approach in which soot is formed either directly from vaporized fuel or from an inception species which in most cases is acetylene. However this requires a detailed chemical model. The most widely used chemical models are based on the work of Frenklach, Wang and co-workers (Frenklach and Wang [21]; Appel et al. [6]). However neither model includes PAH chemistry larger than pyrene and PAH oxidation chemistry. PAH growth and oxidation is an active area of research and a number of more complete models have been published (*e.g.* Mosbach et al. [62]).

The model in Kazakov and Foster [39] is also of empirical nature but represents soot by two numbers, soot mass fraction and particle number. The underlying assumption is that all particles have the same size, *i.e.* the particle size distribution is monodisperse. Assuming particles are only represented by the mass of carbon contained in a particle, one can use statistical moments to describe the particle size distribution. This was done successfully by Frenklach and co-workers and is now widely used in the combustion com-

munity (Frenklach and Wang [21]; Frenklach [20]). Another widespread approach is to classify the particle sizes into bins or sections and describe the time evolution of each section, for example D'Anna and Kent [14] and Lindstedt and Waldheim [56]. An alternative is to represent the particle size distributions by individual stochastic particles and use a Monte Carlo method to simulate their growth and oxidation (Balthasar and Kraft [7]). Both moment and sectional models cannot easily be used in higher dimensional type spaces, *i.e.* when more properties of a particle are of interest. Typical examples are models where the chemical composition and the particle surface are included (Mosbach et al. [62]). Employing some additional simplifications also moment (Blanquart and Pitsch [9]) and sectional models have been used.

Tiny carbon or ash nuclei have been observed in engine exhaust and may act as nucleation sites for semi-volatile nanoparticles of mixed composition. Tiny carbonaceous soot precursors are formed early in the combustion process as shown in Figs. 6(b) and 7(h) but it is unclear if and under what conditions these particles survive the expansion and exhaust processes. None of the current soot models take ash nuclei into account. Formation of nucleation mode particles is discussed in more detail below.

6   Other Processes and Particles

Referring back to Fig. 3 we see that ash particles are formed relatively early in the combustion process. The air shown being entrained into the burning fuel jet shown in Fig. 4 also contains any particulate matter that penetrated the air cleaner, atomized and evaporated lubricating oil, and material blown off from in-cylinder surfaces or left over from previous cycles. Particle formation from metals in engines has been examined by a number of investigators (Abdul-Khalek et al. [2]; Jung et al. [35]; Lee et al. [53]; Miller et al. [61]; Gidney et al. [24]; Gidney et al. [25]; Mayer et al. [59]). Following Abdul-Khalek et al. [2] in order to illustrate the possible fate of a lube oil metal, the chemical equilibrium distribution of Ca compounds from the oil at the edge of the burning fuel jet has been calculated and the results are plotted against temperature in Fig. 10. These calculations were done for oil with 5000 ppm Ca, oil consumption 0.1% of fuel consumption and a diesel fuel with 10 ppm sulfur burning at an equivalence ratio of 1 and pressures of 1 atm and 30 atm. At the highest temperatures most of the Ca is found as gaseous hydroxides, but as products of combustion cool equilibrium shifts first to CaO and then at lower temperature to $CaSO_4$. The exact distribution of Ca compounds will depend on actual reaction rates but these equilibrium calculations suggest that gas to particle conversion is likely to take place as the cylinder gases cool below about 1300 ºC. Whether the resulting materials are emitted as individual nucleation mode particles or are scavenged by soot particles in the accumulation mode depends on the rate of cooling and the concentration of soot. Fast cooling and low soot concentrations favor nucleation. This means that engines with very low soot emissions will emit ash as very small particles in the nucleation mode range (Gidney et al. [24]; [25]). Engine wear generates coarse particles containing metals like Fe and Cu that may be directly emitted or accumulate in the oil. Atomized oil will introduce these metals back into the combustion chamber and a fraction may vaporize and subsequently form nanoparticles (Mayer et al. [59]).
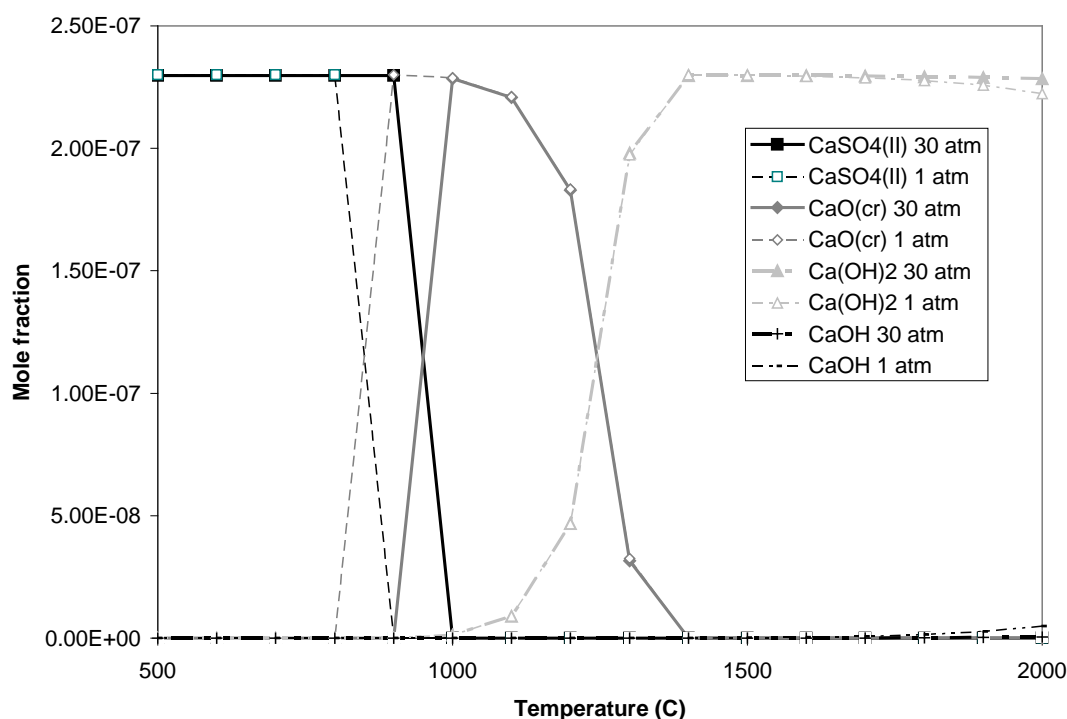
17

Figure 10: *Equilibrium distribution of Ca species for conditions expected during engine expansion stroke. ULSD, 10 ppm sulfur, equivalence ratio = 1, oil consumption 0.1% of fuel consumption, oil composition, mass fraction Ca, S, P. 5000, 5000, and 1000 ppm, respectively.*

In engines fitted with exhaust filters, ash particles are removed from the exhaust but accumulate in the filter and necessitate periodic cleaning. However engines that produce sufficiently low particle emissions to meet emission standards without filters will emit these particles into the atmosphere. As shown in Fig. 3, semi-volatile nucleation mode particles form as the exhaust cools and dilutes. Semi-volatile particle precursors, mainly sulfuric acid and hydrocarbons, become supersaturated and undergo gas-to-particle conversion. Except under very light load and idle conditions, temperatures in the tailpipe are too high for nucleation to occur and most of the nucleation and growth takes place as the exhaust mixes with ambient air, not in the tailpipe. Nucleation is an extremely nonlinear process so that dilution conditions, for example, temperature and dilution rate, may change the concentration of semi-volatile particles in the nucleation mode by an order of magnitude or more. On the other hand, solid particles, mainly carbon agglomerates and ash, are formed in the engine itself and are thus not influenced by dilution conditions.

6.1 Influence of sampling and dilution conditions on particle formation and growth

A number of early studies examined the influence of dilution conditions on nucleation mode formation (Abdul-Khalek et al. [2]; [3]; [4]) and found that most of the nucleation

18

mode formation and growth took place at dilution ratios between about 5 and 20 where the saturation ratio of the semi-volatile particle precursors reaches a maximum. A two-stage sampling and dilution system (VRTDS) was developed consisting of primary dilution, a variable residence time aging chamber where nucleation and growth occurs under controlled conditions, and then secondary dilution to freeze subsequent formation, growth, and coagulation processes. Figure 11 shows the influence of dilution and sampling conditions on the size distributions measured using the VRTDS and an SMPS to measure particle size and concentration (Abdul-Khalek et al. [4]). The results shown are for a medium-duty diesel engine running at medium speed and load. The nucleation mode is strongly influenced by dilution conditions. Increasing residence time in the primary dilution chamber from 230 ms to 1 s increases the number concentration in the nucleation mode by two orders of magnitude. Decreasing the temperature in the primary dilution chamber from 66 °C to 32 °C increases the number concentration in the nucleation mode by about one and a half orders of magnitude.
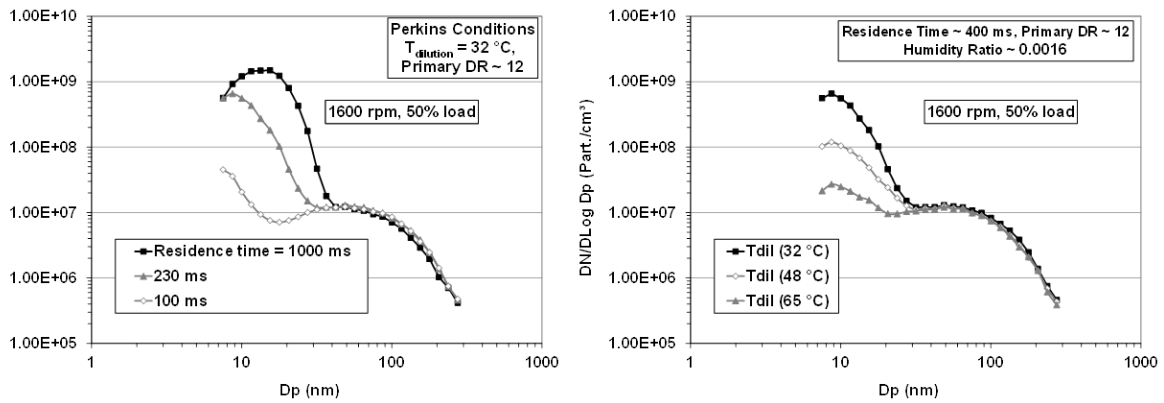

Figure 11: *Influence of dilution conditions on nucleation mode formation. The left panel shows the influence of aging time at fixed dilution ratio, temperature, and humidity. The right panel shows influence of primary dilution temperature at fixed residence time, dilution ratio, and humidity (Adapted from Abdul-Khalek et al. [4]).*

Unlike the nucleation mode, accumulation mode does not appear to be significantly influenced by these changes. However, most of the semi-volatile mass emitted by a diesel engine is typically in the accumulation mode size range, adsorbed on soot particles. Commonly used particle sizing instruments like the TSI Inc. SMPS and Engine Exhaust Particle Sizer (EEPS) and the Cambustion Differential Mobility Spectrometer (DMS500) size particles based on electrical mobility diameter, which depends on the drag of the external envelop of the particle. Particles in the accumulation mode range are generally soot agglomerates with an external area that does not depend strongly on the amount of adsorbed material. Thus, the relative insensitivity of the mobility diameter of accumulation mode particles to dilution conditions does imply that the amount of adsorbed mass is independent of dilution conditions. Sakurai et al. [68], [69] heated size selected particles in the accumulation mode and found that volume changes calculated from changes in mobility diameter were much smaller than mass changes measured with an aerosol centrifuge.

6.2 Diesel exhaust particles in the atmosphere

Concerns about sampling and dilution led to the CRC E-43 program (Kittelson et al. [45]); in which measurements made in the laboratory and under real-world, on-road conditions were compared. A mobile emissions laboratory (MEL) was constructed to determine the relationship between nucleation mode formation under real-world roadway conditions and typical laboratory test conditions. The MEL was used to collect gaseous and aerosol data while following heavy-duty trucks on rural roadways. The sample intake, located in front of the MEL, was set at a height of 4 m to sample the plume of heavy-duty trucks. The primary instrument used to determine the number, surface, and volume size distributions was a TSI 3071 SMPS. It was configured to measure particles in the size range from 8 to 300 nm. A TSI 3025A Ultrafine Condensation Particle Counter (UCPC) (Kesten et al. [40]; Wiedensohler et al. [88]) was used to determine the total number concentration for particles ranging in size from about 3 to 1000 nm. This UCPC has a maximum concentration of 100,000 particles cm^{-3}. Leaky-filter dilutors with dilution ratios ranging from 220:1 to 350:1 were used with the UCPC to prevent overranging. Onboard gas analyzers measured CO_2, CO, and NO_x in the diluted exhaust plume and roadway background. Sensors in the exhaust of the trucks being chased measured CO_2 and NO_x simultaneously and allowed on-road dilution ratios to be calculated. Further details on the MEL and the instruments and systems used are available elsewhere (Kittelson et al. [43]; [45]). The same trucks were tested on chassis dynamometers at the engine manufacturer's facility. Sampling and dilution conditions were optimized to match roadway size distributions as closely as possible (Kittelson et al. [47]).
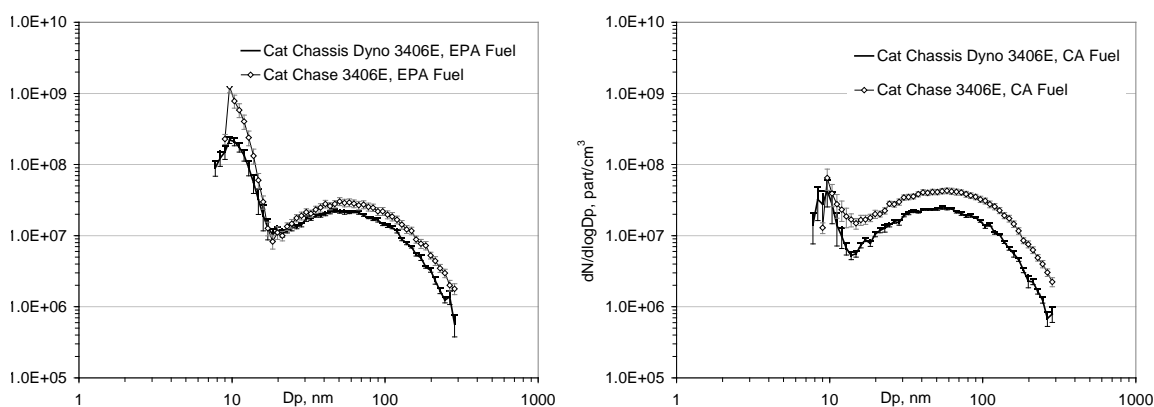
Figure 12: *On-road and laboratory size distributions operating on 350 ppm S EPA fuel, left pane, and 50 ppm S CA fuel, right pane (Adapted from Kittelson et al. [45]).*

Figure 12 shows on-road chase and chassis dynamometer measurements of size distributions for a truck powered by a heavy-duty diesel engine with full electronic engine management and meeting the 0.1 g $bhp^{-1}hr^{-1}$ particulate matter (PM) standard that was in effect from 1994 through 2006. Since 2007 all heavy-duty trucks in the U.S have been fitted with diesel particle filters (DPF) so that this engine is representative of modern pre DPF engine technology. The results shown are a composite of loaded and unloaded high-

way cruise under moderate summer conditions. Results are shown for a CA fuel with about 50 ppm sulfur and an EPA fuel with about 350 ppm sulfur. The CA fuel produced a smaller nucleation mode than EPA fuel. A volatile nucleation mode was present both on-road and in the laboratory. A two-stage, porous tube/ejector dilutor system was used in the laboratory tests on the chassis dynamometer. It could reasonably simulate on-road nucleation mode formation under appropriate test conditions. The size of the nucleation mode relative to the accumulation is more significant than the absolute levels due to uncertainty in on-road dilution ratios. These results and similar ones for other engines tested in the E-43 program show that it is possible to simulate nucleation mode formation for carefully defined on-road conditions. However, at present, it is unclear as to which on-road conditions should be simulated. There are many variables, including temperature, previous operating history, road speed, exhaust system design, and others.

Rönkkö et al. [66] did a similar comparison of exhaust particle size distributions from a heavy-duty diesel engine measured under laboratory and on-road conditions. Dilution was done in the laboratory using a two stage dilution system consisting of a porous wall dilutor followed by an ejector dilutor. On-road size distributions measured in chase experiments stabilized within about 5 m of the exhaust stack. Concentration and size of particles in the accumulation mode agreed well between on-road and laboratory dilution and although the size of particles in the nucleation mode was similar in laboratory and on-road measurements, concentrations were higher in on-road measurements. Low temperature and high humidity increased nucleation mode formation. A similar dependence upon temperature was observed in the E-43 study but humidity effects were less clear.

6.3   Physical and chemical properties of diesel aerosols

A variety of physical and chemical methods were used to characterize the composition and size of diesel particles from contemporary diesel engines without aftertreatment as part of the CRC/DOE E-43 program (Tobias et al. [82]; Ziemann et al. [91]; Sakurai et al. [68], [69]; Kittelson et al. [47],[48]). Particle size distributions were measured for a variety of engines, test conditions, and fuels. Figure 13 shows some representative measurements. The first panel shows the influence of operating conditions on the formation of solid and volatile nucleation modes. At idle and light load large volatile nucleation modes form under normal sampling and dilution conditions. When a catalytic stripper (CS) (Kittelson et al. [46]; Swanson and Kittelson [81]) is used to remove volatile material, a solid nucleation mode remains, especially at idle. For the higher load condition there is no evidence of either a solid or volatile nucleation mode. As the load is increased, the size of the accumulation mode increases, providing surface to scavenge materials that would otherwise form a nucleation mode.

The other three panels, b, c, and d, in Fig. 13 show the influence of fuel sulfur content and operating conditions on the formation of a nucleation mode. Results are shown for fuel sulfur levels varying from 1 to 325 ppm with and without a thermal denuder (TD) that, like the CS, was used to remove volatile material. The TD measurements show a unimodal aerosol with no evidence of a solid nucleation mode. At the two lighter load conditions significant volatile nucleation modes are present at all sulfur levels and their

concentrations increase with the fuel sulfur content. At the highest load condition, no nucleation mode is formed except for the highest fuel sulfur content. This test condition also led to the formation of the largest concentration of accumulation mode particles which act as a sink for semi-volatile materials and suppress nucleation.
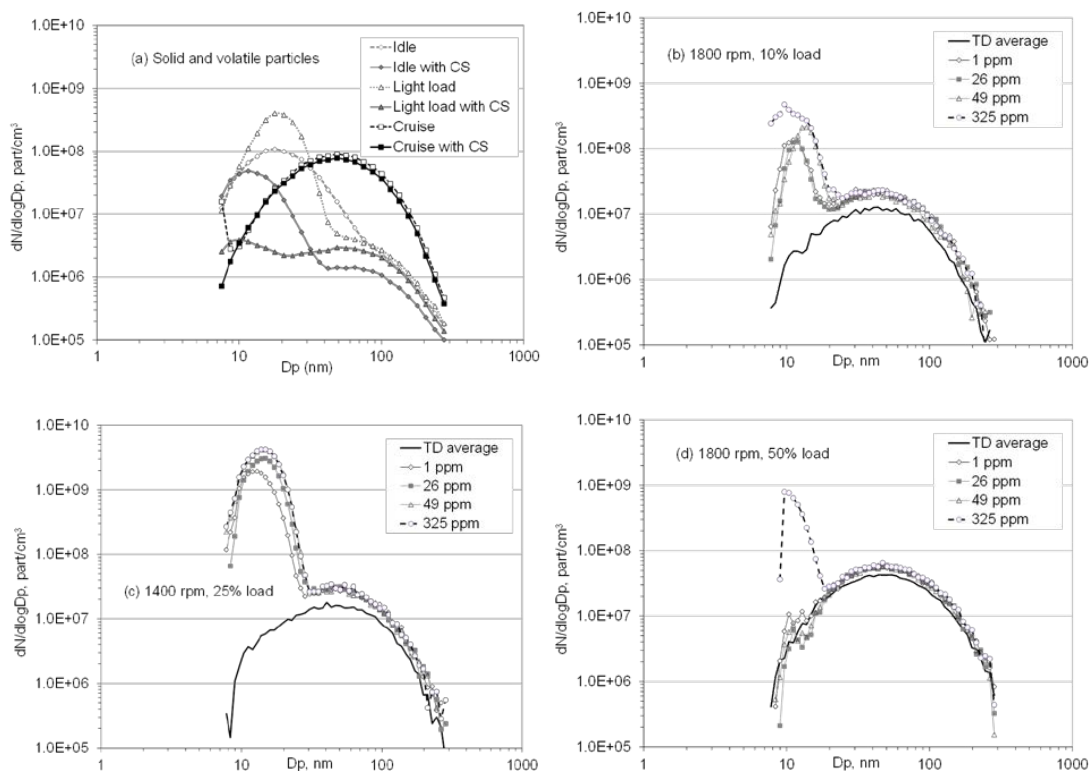

Figure 13: *Influence of operating conditions and fuels on solid and volatile particles. Panel (a) influence of operating conditions on solid and volatile, heavy-duty engine, 50 ppm S fuel, CS denotes catalytic stripper. Panels (b)-(d) (adapted from Kittelson et al. [47]) illustrate the influence of fuel sulfur content on formation of the nucleation mode, heavy-duty engine, zero S fuel doped to S levels from 1 to 325 ppm S, TD denotes thermal denuder.*

A thermal desorption particle beam mass spectrometer (TDPBMS) was used to measure the volatility and mass spectra of the volatile fraction particles in selected size ranges between 15 and 300 nm. Three different engines were tested with fuels of sulfur content ranging from 0 to 360 ppm. The engines were tested under steady state conditions at moderate speeds and loads. For these engines and fuels, the organic component of diesel particles in both the nucleation and accumulation modes appeared to be mainly unburned lubricating oil. The major organic compound classes found were alkanes, cycloalkanes, and aromatics. Low-volatility oxidation products and polycyclic aromatic hydrocarbons that have been found in previous GC-MS analyses (Rogge et al. [65], Schauer et al. [72]) were only a minor component of the organic mass. Unlike traditional methods, the TDPBMS analyzes all of the material that can be thermally desorbed instead of the organic mass that is amenable to speciated analysis that typically constitutes only 5 to 10% of the elutable

organic particulate matter and is thus less sensitive to low concentration species. Small amounts of sulfuric acid could be detected in nanoparticles formed with 360 ppm sulfur fuel, but those formed with less than 100 ppm sulfur fuel showed no evidence of sulfuric acid; these nanoparticles were nearly pure heavy organics.

The physical properties of the particles were studied using Tandem Differential Mobility Analysis (TDMA) originally developed by Rader and McMurry [64]. These experiments allowed size-resolved measurements of volatility to be made. The particles were heated and the diameter decrease measured. These measurements showed that the particles consisted of an external mixture of "more volatile" and "less volatile" particles. At 30 nm, roughly the boundary between the nucleation and accumulation modes, both "more volatile" and "less volatile" particles were found. For smaller sizes, "more volatile" particles like those found in the nucleation mode dominated; for larger sizes, "less volatile" particles like the carbonaceous agglomerates found in the accumulation mode dominated. The "more volatile" particles evaporated in TDMA like C24-C32 normal alkanes. These heavy alkanes are much more prevalent in lubricating oil than in fuel. Taken together, the size distribution, TDPBMS, and TDMA measurements lead to several conclusions about the formation and composition of the nucleation mode. The size distribution measurements show that, in general, increasing the fuel sulfur increases the magnitude of the nucleation mode. On the other hand, the TDPBMS and TDMA measurements show that the nucleation mode consists mainly of heavy hydrocarbons, with a significant amount of sulfuric acid found only in the smallest particles with the highest amount of fuel sulfur. Thus, it would appear that the presence of sulfur in the fuel facilitates the nucleation and growth of nucleation mode particles that consist mainly of heavy hydrocarbons. This same hypothesis was postulated based solely on size distribution measurements and physical arguments by Khalek et al. [42] and later by modeling the physics of nucleation mode formation (Vouitsis et al. [85]).

In most cases, the nucleation mode contains less than 1% of the particle mass. Since diesel particulate matter often contains 10% or more sulfate and water and 20% or more OC, most of the sulfate and OC mass must reside in the accumulation mode, presumably adsorbed on the carbonaceous agglomerates formed by combustion. The nonvolatile material found in the nucleation mode at idle and light load conditions is likely to be ash formed from metallic additives in the lubricating oil, although the presence of tiny solid carbonaceous particles cannot be ruled out.

6.4   Formation and growth of the nucleation mode

The relative importance of homogeneous and heterogeneous nucleation and the role of solid nucleation sites in the formation of the nucleation mode are still unclear. In this paper we have focused on engines without exhaust aftertreatment that were run mainly on relatively high sulfur fuels, often in the 350 ppm S range. Kittelson [44] suggested that for engines without aftertreament running on such fuels the primary nucleation step was binary sulfuric acid water nucleation. Khalek et al. [42] argued that although the primary nucleation step was binary sulfuric acid water, the sulfuric acid concentration in the exhaust was insufficient to explain observed growth rates, that heavy hydrocarbons were

the likely growth species. This explanation is consistent with the observation by Tobias et al. [82] that the nucleation mode consisted of mainly heavy hydrocarbons with a small amount of sulfate. Lemmetty et al. [54] modeled binary sulfuric acid water nucleation in a diluting exhaust plume. They included coagulation and condensation sinks associated with existing soot particles and examined different rates of dilution and cooling. Their model predicted that the sulfuric acid concentration associated with 100% conversion of the sulfur in a 5 ppm sulfur fuel would produce a nucleation rate sufficient to explain observed nucleation mode formation, even when coagulation and condensation sinks corresponding to soot concentrations characteristic of older engines were included. The same sulfuric acid concentration would be produced with a 350 ppm S fuel with a 1.4% conversion rate, a reasonable value for and engine without aftertreatment. This work suggests that homogeneous nucleation of sulfuric acid and water could provide the nucleation sites necessary to explain nucleation mode formation by engines without aftertreatment running on higher sulfur fuels at moderate and higher loads, but not for conditions where the product of the sulfur content of the exhaust and the conversion rate to sulfuric acid is low. Such conditions include light loads with higher sulfur fuels and all load conditions with very low sulfur fuels. Under these conditions other nucleation sites consisting of solid particles or very low volatility hydrocarbons may be important.

The engine studies described above found little evidence of a solid core in nucleation mode particles except at a few light load conditions where a solid ash mode was observed, but in most cases the instruments used in these studies could not resolve particles smaller than 8 nm. However, Ziemann et al. [91] and Sakurai et al. [68] examined particles as small as 3 nm and found some evidence of a solid residue when "more volatile" particles were heated in the TDMA system. Pure lubricating oil particles also produced a solid residue and there was a suggestion of a solid residue when pure normal alkane particles were heated. Thus the solid residue associated with the "more volatile" particles might either represent some type of charring or a true solid residue although Sakurai et al. [68] suggested that diesel nanoparticles are mainly alkanes and would not be expected to char.

Other work has suggested that a solid core might be important. Lähde et al. [51] argued that for engines without catalyzed diesel particle filters (CDPF) but with modern low sulfur fuels, binary homogeneous nucleation of sulfuric acid would be unable to provide sufficient nucleation sites for formation of the nucleation mode. They also examined and ruled out the possibility of ionic nucleation. However they found a small fraction of nucleation mode particles, about 1-2% were charged, suggesting that these particles were formed by heterogeneous nucleation on tiny solid particles formed by combustion, which would be expected to be charged. They also directly measured tiny solid particles with concentrations nearly the same as the nucleation mode particles providing further evidence that the nucleation mode was formed by heterogeneous nucleation.

De Filippo and Maricq [15] also found evidence of a solid core in nucleation mode particles emitted by engines without a CDPF. They tested three different light duty engines and measured the charged fraction as a function of particle size and size distributions with and without a thermal denuder (TD) to remove volatile particles. At idle, one of the engines showed little evidence of a solid nucleation mode but the other two engines, based

both the charged fraction and TD measurements, gave results consistent with formation of nucleation mode particles by heterogeneous nucleation on solid particles formed by combustion. They also examined the morphology of the nucleation mode particles by electron microscopy and found that they exhibited a diffuse amorphous structure similar to soot precursor particles observed in some flame studies.

Rönkkö et al. [67] tested a heavy-duty Euro IV engine without aftertreatment under various dilution and sampling conditions with and without a TD. Their results were essentially independent of fuel sulfur content and suggest that the nucleation mode consisted mainly of heavy hydrocarbons that had undergone heterogeneous nucleation on a solid core. The engine they tested had very low soot emissions relative to OC emissions, which were assumed to derive mainly from partially burned lubrication oil. This led to the formation large concentrations of nucleation mode particles because soot levels were insufficient to adsorb the hydrocarbons and thus suppress nucleation. The high oil to soot ratio would make it more likely that lubricating oil ash particles form a separate nucleation mode as suggested earlier in the discussion of Fig. 3. Thus nucleation mode particles formed from lubricating oil ash may have provided sites for nucleation of heavy hydrocarbons.

A different nucleation path is suggested by Inoue et al. [31]. They used time of flight secondary ion mass spectrometry (TOF-SIMS) and metal assisted SIMS to analyze volatile nanoparticles formed by a light duty diesel engine under idle and deceleration conditions. They suggest that at under these lighter load conditions low volatility hydrocarbon species are the nucleating materials: oxygenated hydrocarbons at idle and high molecular weight hydrocarbons >C35 during deceleration.

Thus, available studies suggest that for engines without aftertreatment different primary nucleation steps may be involved, depending on engine conditions and fuel. An important unresolved question is the presence of a solid core. Most modern engines are equipped with CDPFs which are very efficient in removing solid particles, especially in the nanometer range where diffusion is a very effective removal mechanism. However improved combustion may make it possible to meet emission standards without aftertreatment (see Auto131 particulate matter aftertreatment discussions). Then any extremely tiny particles present will be emitted to the atmosphere with possible negative health impacts.

7 Particle Emissions from Gasoline Engines

The previous sections focused on particle emission in diesel engines. However most of the light duty vehicles operate either port fuel injected (PFI) or direct injected gasoline engines (DISI). Although modern, well maintained PFI engines emit very little PM in certification driving cycles, older and worn engines and engines operating under high load or cold start conditions can emit significant amounts of PM. For example, Storey et al. [80] tested a pristine 1967 (pre emission control vehicle, designed for leaded fuel) in the standard US FTP cycle and found it emitted 41 mg/mi when operated on modern unleaded fuel and 140 mg/mi when operated on leaded fuel. More recently the Kansas City Light-Duty Vehicle Emission Study (Fulper et al. [23]) was initiated because of ongoing

uncertainty about the relative contributions of diesel and gasoline vehicles to PM2.5. Vehicles were tested on a portable chassis dynamometer under outdoor ambient temperature conditions using the LA92 Unified Cycle. Tests were conducted in a summer phase in 2004 with a fleet consisting 80 light trucks and 181 passenger cars, and a winter phase in 2005 with a fleet consisting of 119 light trucks and 116 cars. PM emissions ranged over three orders of magnitude with a downward trend for newer vehicles. The median PM emissions for cars in the summer tests were 45, 7, 5, and 2 mg/mi for the pre 1981, 81-90, 91-95, and post 1996 model years, respectively. To put this into context, the emission standards for 1992-95, 96-99, and 2000-04 European diesel passenger cars were 220, 130 and 80 mg/mi. While these results indicate much higher PM emissions from diesels, in-use and certification tests are not strictly comparable because PM emissions from PFI engines are much more dependent on operating conditions than those from diesel engines. The dramatic drop in emissions between pre-1981 cars and later years is likely associated with the introduction of three-way catalysts and associated closed loop fuel-air ratio control. PM emissions from PFI engines have been shown to increase significantly on cold starts and to be strongly fuel-air ratio and load dependent (Abdul-Khalek and Kittelson [1], 1995; Graskow et al. [26]; Maricq et al. [57]; Kittelson et al. [47]; Schauer et al. [73]). The fuel system on a 3-way catalyst equipped PFI vehicle delivers an essentially chemically correct homogeneous mixture to the cylinder under normal driving conditions leading to very low PM emissions. However, much richer mixtures are used under cold start and some high load conditions leading to local inhomogeneities associated with incomplete fuel evaporation, wall wetting, pool burning and much higher PM emissions.

More recently PFI technology is being replaced by gasoline direct injection (GDI) (Kume et al. [50]; Iwamoto et al. [32]; Yi et al. [89]; McMahon et al. [60]; CARB [12]) in which the gasoline is directly injected into the cylinder rather than into the inlet manifold. These engines have been available in Japan and Europe since the 1990s and started entering the US market in 2003. EPA projects that they will account for 50% of the gasoline vehicle market in the U.S by 2020 (CARB [12]).

While GDI technology can lead to improved fuel economy, particle emissions often exceed that of PFI engines. GDI engines may operate in a stratified charge, lean mode or in a homogeneous charge, stoichiometric mode. In the stratified lean mode the fuel is injected late in the compression stroke and the diluting fuel jet is transported toward the spark plug by in-cylinder motion. Like a diesel, combustion takes place in and around the diluting fuel jet, but gasoline is much more volatile than diesel fuel so evaporation and mixing are faster. Unlike a diesel, ignition occurs at a spark plug rather than by autoignition. In the homogeneous stoichiometric mode, fuel is injected early in the intake stroke so that there is sufficient time for mixing and formation of a homogeneous mixture. Lean GDI engines generally use late injection for stratified lean operation at light load and early injection for homogeneous charge stoichiometric at heavier loads, while stoichiometric engines use early injection throughout their operating range. Another important characteristic of GDI engines is the means of obtaining and controlling charge stratification. The mixing and motion and the fuel jet may be, wall-guided, spray guided, or air guided. Most early GDI engines used a wall guided mixing while more recently spray guided systems are becoming more common. Few attempts have been made to model particle emissions in GDI

engines using a detailed soot model. For example, Etheridge et al. [18]) simulates the soot particle sized distribution in a GDI engine with early injection. Although the model was able to reproduce qualitative trends it uses an empirical model for flame propagation which has to be calibrated.

Two mechanisms have been identified to contribute to the formation of soot formation in GDI engines. Firstly, stratification of the charge leads to rich-burning zones in the fuel jet that produce soot particles and secondly fuel spray that strikes the piston will form liquid films and pools and the resulting pool fires produce significant amounts of PM and HC. In lean GDI engines, lean mixtures and minimized throttling lead to better fuel economy but both stratification of the charge and pool burning lead to soot formation. Gaseous emission control is complex utilizing both a lean NO_x trap in lean operation and a three-way catalyst in stoichiometric operation. Stoichiometric GDI engines use early injection to minimize stratification but large droplets and spray impingement still lead to more soot formation than in PFI engines. While PFI engines also form soot related to large droplets and pool burning, fuel is generally injected against closed intake valves where it evaporates and any remaining liquid is effectively atomized by shearing action of air flowing over the intake valves early in the intake stroke. Stoichiometric operation allows a 3-way catalyst to be used for CO, hydrocarbon and NO_x control.

Andersson et al. [5] tested a range recent diesel and gasoline passenger cars as part of the EU PMP program: 6 DPF equipped diesel, 6 conventional diesel, 3 PFI, 3 lean GDI, and 1 stoichiometric GDI. Number (PN) emissions for the lean GDI vehicles were about one and a half orders of magnitude higher than PFI vehicles and one and a half orders of magnitude lower than conventional diesel. The stoichiometric GDI vehicle PN emissions were about a factor of 4 lower than lean GDI vehicle. As a group DPF equipped diesels produced the lowest emission, slightly lower than PFI gasoline. The cleanest of the lean GDI engines used spray guided combustion systems and produced PM emissions in the range of 2-2.5 mg/km, easily meeting the Euro 6 PM emission standard of 4.5 mg/km. On the other hand PN emissions ranged from 2 to 4 x 10^{12} particles/km, 3 to 7 times the Euro 6 PN standard of 6 x 10^{11} particles/km that applies the diesel vehicles. Braisher et al. [10] found that a lean GDI vehicle produced PN and PM emissions about half and order of magnitude higher than a stoichiometric GDI vehicle which in turn produced PN and PM emissions about an order of magnitude higher than a PFI vehicle when tested over the New European Driving Cycle. The cleanest GDI vehicle used a stoichiometric wall guided combustion but produced PM emission slightly above the Euro 6 standard and PN emissions 10 times the diesel standard. These high particle emissions have prompted several studies on the effects of engine operating parameters and fuel composition on particle characteristics. Khalek et al. [41] tested a 2009 stoichiometric GDI engine on 3 commercially available fuels. Emissions ranged from 0.7 to 3.2 mg/km and 2 to 5.9 x 10^{12} particle/km on the FTP cycle and 1.3 to 12.8 mg/km and 4.2 to 15.9 x 10^{12} particle/km on the more aggressive US06 cycle. Somewhat surprisingly the highest emitting fuel was the only one containing ethanol (E10 or 10% ethanol by volume) which usually reduces particle emissions. However, other properties of the fuel were also different. Maricq et al. [58] tested the influence of engine calibration and ethanol content of the fuel on the gaseous and particle emissions from a current technology stoichiometric GDI vehicle. With neat

gasoline (E0) PM emissions ranged from 1.9 to 4.3 mg/km depending on engine calibration. E10 and E17 produced roughly 20% reductions in PM but the changes were within experimental uncertainty. Higher blends, E32 and E45 produced a statistically significant decrease in PM of about 45% compared E0. Storey et al. [79] examined the influence of ethanol blends on particle emissions from a Euro 4 lean spray guided GDI vehicle and a 2007 US stoichiometric GDI vehicle. Tests were run for a variety of conditions including US FTP and US06 cycles, steady state, and step transient tests. Fuels tested included E0, E10 and E20. In the FTP cycle emissions of PM with the E0 fuel were 2 and 2.8 mg/km for stoichiometric and lean, respectively, while in the US06 cycle PM emissions for the two vehicles were similar at about 3.3 mg/km. Ethanol blends led to significant PM reductions in the range of 50% for E20 blends. Zhang and McMahon [90] tested a fleet of 9 2007 to 2010 stoichiometric GDI light duty vehicles, 7 with wall guided and 2 with spray guided mixing. A 2009 PFI vehicle was also tested. The test fuel was a standard California summer blend containing 6% ethanol. The vehicles were tested on the FTP cycle and PM emissions ranged from 1 to 5.3 mg/km for the GDI vehicles and 0.4 mg/km for the PFI vehicle. As a group the spray guided GDIs were cleaner than the wall guided with PM of 1.5 compared to 2.7 mg/km but the PM emissions from the best spray and wall guided were essentially the same at 1.0 mg/km. PN emissions from the best spray and wall guided vehicles were 2.8 and 1.9 x 10^{12} particles/km, so that for PN the wall guided system was actually better. The authors attribute this to very high emissions during the cold start but low emissions subsequently with the spray guided system while the wall guided system did not produce such high cold start emissions but continued to emit at moderate levels throughout the cycle.

The bulk composition of GDI particles was examined in several of these studies (Andersson et al. [5]; Khalek et al. [41]; Storey et al. [79]; and Maricq et al. [58]). The composition of particles from lean GDI is similar to diesel, a mix of organic carbon (OC) and elemental carbon (EC) with typically more EC than OC. Stoichiometric GDI engines have high exhaust temperatures and a 3-way catalyst that oxidizes most of the OC leaving mainly EC. With stoichiometric engines OC does not depend very much on the fuel and is likely associated with high molecular weight components associated the lubricating oil. In lean engines the addition of ethanol to the fuel reduces the EC and slightly reduces the OC while in stoichiometric engines it strongly reduces EC but has little impact on OC. This suggests EC is fuel derived and some OC is fuel derived in lean engines, but OC is largely fuel independent in stoichiometric engines, presumably derived mainly from heavy ends of the lube oil that pass through the catalyst. Earlier work on the performance of three-way and oxidizing catalysts on high molecular weight organic components showed that it is diffusion limited so that high molecular weight, low diffusion coefficient components may pass through a catalyst that is otherwise very effective (Johnson and Kittelson [33]; Graskow et al. [26]).

The morphology of particles from a stoichiometric GDI engine was examined by Seong et al. [74] using high resolution transmission electron microscopy. Particles were sampled using a thermophoretic sampler upstream of the three-way catalyst. Fractal analysis of the aggregates showed that the compactness was intermediate between those from light-duty and heavy duty diesel engines. The primary particles in the aggregates had graphitic struc-

tures but were less ordered than typical of diesel particles. Primary particles under 10 nm diameter were observed under some conditions.

GDI particle emissions are sensitive to many factors, lean vs stoichiometric, spray vs wall guided, calibration details and fuels. The response to ethanol containing fuels illustrates the complexity of the problem, Storey et al. [79] showing large reductions in PM with E20, Maricq et al. [58] showing a much more modest decreases, and Khalek et al. [41] showing an increase with E10, although in this case other fuel properties were also different. Particle emissions from GDI engines, both in terms of PM and PN fall between those from diesel and those from PFI gasoline. GDI engines have less soot forming tendency than diesel because the fuel is more volatile and more resistant to autoignition so that the fuel jet mixes to a leaner mixture before ignition occurs, but more of a tendency to form soot than PFI because although the fuel jet is better mixed at combustion than in a diesel, it is still not as homogeneous as the charge formed by vaporization in the intake port and atomization by the shearing flow over the intake valve that takes place in a PFI engine. The GDI fuel spray is also more prone to wall wetting and pool burning especially on cold starts where vaporization is slow.

Progress is being made in reducing both PM and PN emissions from GDI vehicles but significant challenges remain. Most of the vehicles tested recently would meet the Euro 6 PM standard of 4.5 mg/km and the cleanest could already meet the proposed 2017 California LEV III standard of 1.9 mg/km. However, none of them could meet the Euro 6 diesel PN standard of 6 x 10^{11} particles/km. A PN standard for GDI vehicles goes into effect in September 2014, but to allow time for further development the EU will allow GDI vehicles to emit 6 x 10^{12} particles/km, 10 times the diesel level until September 2017 when the standard drops to the diesel level. At present there are no plans for a PN standard in the US.

8 Challenges and Future Research Needs

All processes which lead to particle formation as they have been described above are still not understood well enough to create a truly predictive overall model of particle formation in internal combustion engines. In the following an attempt is made to highlight the most important needs in different areas.

Spray: For the development of better spray models it is necessary that the flow of the liquid in the nozzle, the influence of the nozzle geometry and the breakup of a spray of varying composition is better understood. This will require high resolution direct numerical simulations and experiments to extract statistics of droplet distributions as a function of injector geometry, injection pressure and composition of the fuel.

Combustion chemistry: The prerequisite of a detailed soot model is a detailed understanding of the combustion chemistry. Combustion chemistry models of the future need to be able to account for realistic fuels using surrogate species which not only reproduce the correct heat release but also include the most important soot precursor reactions to

represent the sooting propensity of practical fuels. For these models to be usable in engine simulation software they have to be sufficiently small, which requires good reduction techniques. To model particulate emission in general the combustion chemistry of the inorganic components needs to be developed.

Soot: None of the existing soot models have predictive power as most of the steps which form, grow, restructure and oxidize soot are not understood. In future computational chemistry, such as molecular modeling and kinetic Monte Carlo studies will guide the model development. It is clear that at least in the first instance very detailed type-space models will be required to understand the restructuring and fragmentation of soot particles. This means that the composition as well as the aggregate structure of the particles needs to be included in a soot model.

Mixing and flow: The flow in an engine is highly turbulent and this will have a profound effect on the speed at with which chemical reactions can occur. The development of LES codes and suitable reaction rate closures may lead to more robust models.

Other particles: Other than soot, three main types of particles emitted are by engines without aftertreatment: (1) metal compounds from additives in the lubricating oil and fuel and from engine wear; (2) semi-volatile hydrocarbons from incomplete combustion of the lubricating oil and fuel - these species consist mainly of alkanes, cycloalkanes, and aromatics, along with smaller concentrations of low-volatility oxidation products and PAHs; and (3) sulfates from fuel and lubricating oil sulfur. As improved combustion processes lead to reduced soot emissions these other particle type will become more important. Lubricating oil is an important source of these other particles and efforts should be made to reduce lubricating oil consumption and metal content. When soot is reduced, less surface area is available to scavenge ash nuclei and more solid ash nanoparticles are likely to be emitted. In engines without particle filters this may become an issue in the future. So far, very little progress has been made to account for these processes in current engine emission models.

Data: As the capabilities to store data have increased, the calibration methods, which have been used so far, need to be developed further to exploit the wealth of available information. In particular, techniques developed for calibrating the control unit, may be used to develop semi-empirical models, which can then be used to improve overall engine performance employing mathematical optimization techniques.

9   Conclusions

Modern experimentation and increasing computing power have contributed much towards the understanding of particle formation in internal combustion engines. In this article we have reviewed work in this area with an emphasis on soot formation during in-cylinder combustion for both diesel and gasoline engines. Aerosols are formed during combustion, in the exhaust duct and post-tailpipe. Specific mechanisms, which play an important role in the formation of aerosols, are injection of fuel, formation and oxidation of parti-

cles during combustion, exhaust gas recirculation (EGR) and condensation of volatiles. The physical and chemical properties of fuels play an important role as they influence ignition behavior as a consequence of mixture preparation in the cylinder and through their different sooting propensity. The mechanisms of formation, growth and oxidation of carbonaceous particles have been discussed in detail and the most popular mathematical modeling approaches were outlined. Solid and semi-volatile nucleation mode particles have been treated in some detail. Except for sulfate particles these particles are effectively controlled by modern catalyzed diesel particle filters, but without filter they will continue to be an issue. Key drivers in the formation of these particles are lubricating oil metals and sulfur in the fuel and oil. Emissions from GDI engines fall in number and mass of particles emitted in between PFI gasoline and diesel engines. Without particle filter technology current GDI engines fall short of the Euro 6 diesel PN standard. Although substantial progress has been made, further model improvement and experimental work is necessary to fully understand the complex processes that lead to aerosol emissions and to improve current technology.

Acknowledgements

References

[1] I. S. Abdul-Khalek and D. Kittelson. Real Time Measurement of Volatile and Solid Exhaust Particles Using a Catalytic Stripper. *SAE Technical Paper 950236*, 1995. doi:10.4271/950236.

[2] I. S. Abdul-Khalek, D. B. Kittelson, and F. Brear. Diesel Trap Performance: Particle Size Measurements and Trends. *SAE Technical Paper 982599*, 1998. doi:10.4271/982599.

[3] I. S. Abdul-Khalek, D. B. Kittelson, B. R. Graskow, Q. Wei, and F. Bear. Diesel Exhaust Particle Size: Measurement Issues and Trends. *SAE Technical Paper 980525*, 1998. doi:10.4271/980525.

[4] I. S. Abdul-Khalek, D. B. Kittelson, and F. Brear. The Influence of Dilution Conditions on Diesel Exhaust Particle Size Distribution Measurements. *SAE Technical Paper 1999-01-1142*, 1999. doi:10.4271/1999-01-1142.

[5] J. Andersson, M. Keenan, and K. Akerman. GDI particles-Legislation, current levels and control. *Ricardo Presentation, RD. 09/99801.1, accessed January 19, 2014*, 2008. URL http://www.cambridgeparticlemeeting.org/sites/default/files/Presentations/2009/JAndersson(Ricardo)_2009_GDI_PM.pdf.

[6] J. Appel, H. Bockhorn, and M. Frenklach. Kinetic Modeling of Soot Formation with Detailed Chemistry and Physics: Laminar Premixed Flames of C2 Hydrocarbons. *Combustion and Flame*, 121(1-2):122–136, 2000. doi:10.1016/S0010-2180(99)00135-2.

[7] M. Balthasar and M. Kraft. A stochastic approach to calculate the particle size distribution function of soot particles in laminar premixed flames. *Combustion and Flame*, 133(3):289–298, 2003. doi:10.1016/S0010-2180(03)00003-8.

[8] L. Benbrahim-Tallaa, R. A. Baan, Y. Grosse, B. Lauby-Secretan, F. El Ghissassi, V. Bouvard, N. Guha, D. Loomis, and K. Straif. Carcinogenicity of diesel-engine and gasoline-engine exhausts and some nitroarenes. *The Lancet Oncology*, 13(7): 663–664, 2012. doi:10.1016/S1470-2045(12)70280-2.

[9] G. Blanquart and H. Pitsch. Analyzing the effects of temperature on soot formation with a joint volume-surface-hydrogen model. *Combustion and Flame*, 156(8):1614–1626, 2009. doi:10.1016/j.combustflame.2009.04.010.

[10] M. Braisher, R. Stone, and P. Price. Particle Number Emissions from a Range of European Vehicles. *SAE Technical Paper 2010-01-0786*, 2010. doi:10.4271/2010-01-0786.

[11] H. F. Calcote and D. M. Manos. Effect of Molecular Structure on Incipient Soot Formation. *Combustion and Flame*, 49(1-3):289–304, 1983. doi:10.1016/0010-2180(83)90172-4.

[12] CARB 2011. LEV III PM, 2011. Technical Support Document, Development of Particulate Matter Mass Standards For Future Light-Duty Vehicles, California Air Resources Board. Dec. 2011.

[13] D. Chen, Z. Zainuddin, E. Yapp, J. Akroyd, S. Mosbach, and M. Kraft. A fully coupled simulation of PAH and soot growth with a population balance model. *Proceedings of the Combustion Institute*, 34(1):1827–1835, 2013. doi:10.1016/j.proci.2012.06.089.

[14] A. D'Anna and J. H. Kent. Modeling of particulate carbon and species formation in coflowing diffusion flames of ethylene. *Combustion and Flame*, 144(1-2):249–260, 2006. doi:10.1016/j.combustflame.2005.07.011.

[15] A. De Filippo and M. M. Maricq. Diesel nucleation mode particles: Semivolatile or solid? *Environmental Science and Technology*, 42 (21):7957–7962, 2008.

[16] J. E. Dec. A Conceptual Model of DI Diesel Combustion Based on Laser Sheet Imaging. *SAE Technical Paper 970873*, (412), 1997. doi:10.4271/970873.

[17] P. Eastwood. *Particulate Emissions from Vehicles*. ISBN 9780470724552. Wiley-Professional Engineering Publishing Series, 2008.

[18] J. E. Etheridge, S. Mosbach, M. Kraft, H. Wu, and N. Collings. Modelling soot formation in a DISI engine. *Proceedings of the Combustion Institute*, 33(2):3159–3167, 2011. doi:10.1016/j.proci.2010.07.039.

[19] P. F. Flynn, R. P. Durrett, G. L. Hunter, A. O. zur Loye, O. C. Akinyemi, J. E. Dec, and C. K. Westbrook. Diesel Combustion: An Integrated View Combining Laser Diagnostics, Chemical Kinetics, And Empirical Validation. *SAE Technical Paper 1999-01-0509*, 1999. doi:10.4271/1999-01-0509.

[20] M. Frenklach. Method of moments with interpolative closure. *Chemical Engineering Science*, 57(12):2229–2239, 2002. doi:10.1016/S0009-2509(02)00113-6.

[21] M. Frenklach and H. Wang. Detailed Modeling of Soot Particle Nucleation and Growth. *Symposium (International) on Combustion*, 23(1):1559–1566, 1990. doi:10.1016/S0082-0784(06)80426-1.

[22] M. Frenklach, D. W. Clary, W. C. Gardiner Jr, and S. E. Stein. Detailed Kinetic Modeling of Soot Formation in Shock-Tube Pyrolysis of Acetylene. *Symposium (International) on Combustion*, 20(1):887–901, 1985. doi:10.1016/S0082-0784(85)80578-6.

[23] C. R. Fulper, S. Kishan, R. W. Baldauf, M. Sabisch, J. Warila, E. M. Fujita, C. Scarbro, W. S. Crews, R. Snow, P. Gabele, R. Santos, E. Tierney, and B. Cantrell. Methods of Characterizing the Distribution of Exhaust Emissions from Light-Duty, Gasoline-Powered Motor Vehicles in the U.S. Fleet. *Journal of the Air & Waste Management Association*, 60(11):1376–1387, 2010. doi:10.3155/1047-3289.60.11.1376.

[24] J. T. Gidney, N. Sutton, M. V. Twigg, and D. B. Kittelson. Exhaust Inorganic Nanoparticle Emissions From Internal Combustion Engines, in Internal Combustion Engines: Performance, Fuel Economy and Emissions. *Chandos Publishing, Oxford*, pages 133 – 146, 2009.

[25] J. T. Gidney, M. V. Twigg, and D. B. Kittelson. Effect of Organometallic Fuel Additives on Nanoparticle Emissions from a Gasoline Passenger Car. *Environmental science & technology*, 44(7):2562–9, 2010. doi:10.1021/es901868c.

[26] B. R. Graskow, D. B. Kittelson, M. R. Ahmadi, and J. E. Morris. Exhaust Particulate Emissions from Two Port Fuel Injected Spark Ignition Engines. *SAE Technical Paper 1999-01-1144*, 1999. doi:10.4271/1999-01-1144.

[27] K. J. Higgins, H. Jung, D. B. Kittelson, J. T. Roberts, and M. R. Zachariah. Kinetics of Diesel Nanoparticle Oxidation. *Environmental science & technology*, 37(9): 1949–54, 2003. doi:10.1021/es0261269.

[28] H. Hiroyasu and T. Kadota. Models for Combustion and Formation of Nitric Oxide and Soot in DI Diesel Engines. *SAE Technical Paper 760129*, 1976. doi:10.4271/760129.

[29] K. H. Homann. Formation of Large Molecules, Particulates and Ions in Premixed Hydrocarbon Flames; Progress and unresolved questions. *Symposium (International) on Combustion*, 20(1):857–870, 1985. doi:10.1016/S0082-0784(85)80575-0.

[30] R. A. Hunt. Relation of Smoke Point to Molecular Structure. *Industrial & Engineering Chemistry*, 45(3):602–606, 1953. doi:10.1021/ie50519a039.

[31] M. Inoue, A. Murase, M. Yamamoto, and S. Kubo. Analysis of volatile nanoparticles emitted from diesel engine using TOF-SIMS and metal-assisted SIMS (MetA-SIMS). *Applied Surface Science*, 252(19):7014–7017, 2006. doi:10.1016/j.apsusc.2006.02.169.

[32] Y. Iwamoto, K. Noma, O. Nakayama, T. Yamauchi, and H. Ando. Development of Gasoline Direct Injection Engine. *SAE Technical Paper 970541*, 1997. doi:10.4271/970541.

[33] J. E. Johnson and D. B. Kittelson. Deposition, diffusion and adsorption in the diesel oxidation catalyst. *Applied Catalysis B: Environmental*, 10(1-3):117–137, 1996. doi:10.1016/0926-3373(96)00027-6.

[34] D. Jung and D. N. Assanis. Multi-Zone DI Diesel Spray Combustion Model for Cycle Simulation Studies of Engine Performance and Emissions. *SAE Technical Paper 2001-01-1246*, 2001. doi:10.4271/2001-01-1246.

[35] H. Jung, D. B. Kittelson, and M. R. Zachariah. The influence of a cerium additive on ultrafine diesel particle emissions and kinetics of oxidation. *Combustion and Flame*, 142(3):276–288, 2005. ISSN 00102180. doi:10.1016/j.combustflame.2004.11.015.

[36] H. Jung, D. B. Kittelson, and M. R. Zachariah. Characteristics of SME biodiesel-fueled diesel particle emissions and the kinetics of oxidation. *Environmental science & technology*, 40(16):4949–55, 2006. doi:10.1021/es0515452.

[37] G. T. Kalghatgi, L. Hildingsson, A. J. Harrison, and B. Johansson. Autoignition quality of gasoline fuels in partially premixed combustion in diesel engines. *Proceedings of the Combustion Institute*, 33(2):3015–3021, 2011. doi:10.1016/j.proci.2010.07.007.

[38] T. Kamimoto and M. Bae. High Combustion Temperature for the Reduction of Particulate in Diesel Engines. *SAE Technical Paper 880423*, 1988. doi:10.4271/880423.

[39] A. Kazakov and D. E. Foster. Modeling of Soot Formation During DI Diesel Combustion Using a Multi-Step Phenomenological Model. *SAE Technical Paper 880423*, (724), Oct. 1998. doi:10.4271/982463.

[40] J. Kesten, A. Reineking, and J. Porstendörfer. Calibration of a TSI Model 3025 Ultrafine Condensation Particle Counter. *Aerosol Science and Technology*, 15(2): 107–111, 1991. doi:10.1080/02786829108959517.

[41] I. Khalek, T. Bougher, and J. Jetter. Particle Emissions from a 2009 Gasoline Direct Injection Engine Using Different Commercially Available Fuels. *SAE International Journal of Fuels and Lubricants*, 3(2):623–637, 2010. doi:10.4271/2010-01-2117.

[42] I. A. Khalek, D. B. Kittelson, and F. Brear. Nanoparticle Growth During Dilution and Cooling of Diesel Exhaust: Experimental Investigation and Theoretical Assessment. *SAE Technical Paper 2000-01-0515*, (724), 2000. doi:10.4271/2000-01-0515.

[43] D. Kittelson, J. Johnson, W. Watts, Q. Wei, M. Drayton, D. Paulsen, and N. Bukowiecki. Diesel Aerosol Sampling in the Atmosphere. *SAE Technical Paper 2000-01-2212*, (724), 2000. doi:2000-01-2212.

[44] D. B. Kittelson. Engines and nanoparticles: a review. *Journal of Aerosol Science*, 29(5-6):575–588, 1998. doi:10.1016/S0021-8502(97)10037-4.

[45] D. B. Kittelson, W. F. Watts, and J. P. Johnson. Diesel Aerosol Sampling Methodology - CRC E-43 Final Report. *Coordinating Research Council, Alpharetta, GA*, page 181, 2002, accessed January 19, 2014. URL http://www.crcao.com/.

[46] D. B. Kittelson, W. F. Watts, J. C. Savstrom, and J. P. Johnson. Influence of a catalytic stripper on the response of real time aerosol instruments to diesel exhaust aerosol. *Journal of Aerosol Science*, 36(9):1089–1107, 2005. doi:10.1016/j.jaerosci.2004.11.021.

[47] D. B. Kittelson, W. F. Watts, and J. P. Johnson. On-road and laboratory evaluation of combustion aerosols–Part1: Summary of diesel engine results. *Journal of Aerosol Science*, 37(8):913–930, 2006. doi:10.1016/j.jaerosci.2005.08.005.

[48] D. B. Kittelson, W. F. Watts, J. P. Johnson, J. J. Schauer, and D. R. Lawson. On-road and laboratory evaluation of combustion aerosols–Part 2:. *Journal of Aerosol Science*, 37(8):931–949, 2006. doi:10.1016/j.jaerosci.2005.08.008.

[49] M. Kraft. Modelling of particulate processes. *Kona, Powder and Particle*, 23:18–35, 2005.

[50] T. Kume, Y. Iwamoto, K. Iida, M. Murakami, K. Akishino, and H. Ando. Combustion Control Technologies for Direct Injection SI Engine. *SAE Technical Paper 960600*, (412), 1996. doi:10.4271/960600.

[51] T. Lähde, T. Rönkkö, A. Virtanen, T. J. Schuck, L. Pirjola, K. Hämeri, M. Kulmala, F. Arnold, D. Rothe, and J. Keskinen. Heavy Duty Diesel Engine Exhaust Aerosol Particle and Ion Measurements. *Environmental science & technology*, 43(1):163–8, 2009. doi:10.1021/es801690h.

[52] A. A. Lall and M. R. Zachariah. Size resolved soot oxidation kinetics. In Combustion Generated Fine Carbonaceous Particles, H. Bockhorn, A. D'Anna, A. Sarofim, H. Wang. (Eds.). *KIT Scientific Publishing*, pages 501–532, 2009.

[53] D. Lee, A. Miller, D. Kittelson, and M. R. Zachariah. Characterization of metal-bearing diesel nanoparticles using single-particle mass spectrometry. *Journal of Aerosol Science*, 37(1):88–110, 2006. doi:10.1016/j.jaerosci.2005.04.006.

[54] M. Lemmetty, L. Pirjola, J. Mäkelä, T. Rönkkö, and J. Keskinen. Computation of maximum rate of water–sulphuric acid nucleation in diesel exhaust. *Journal of Aerosol Science*, 37(11):1596–1604, 2006. doi:10.1016/j.jaerosci.2006.04.003.

[55] J. S. Lighty, V. Romano, and A. F. Sarofim. Soot oxidation. In Combustion Generated Fine Carbonaceous Particles, H. Bockhorn, A. D'Anna, A. Sarofim, H. Wang. (Eds.). *KIT Scientific Publishing*, pages 487–500, 2009.

[56] R. P. Lindstedt and B. B. O. Waldheim. Modeling of soot particle size distributions in premixed stagnation flow flames. *Proceedings of the Combustion Institute*, 34(1): 1861–1868, 2013. doi:10.1016/j.proci.2012.05.047.

[57] M. M. Maricq, D. H. Podsiadlik, and R. E. Chase. Gasoline Vehicle Particle Size Distributions:Ââ Comparison of Steady State, FTP, and US06 Measurements. *Environmental Science & Technology*, 33(12):2007–2015, 1999. doi:10.1021/es981005n.

[58] M. M. Maricq, J. J. Szente, and K. Jahr. The Impact of Ethanol Fuel Blends on PM Emissions from a Light-Duty GDI Vehicle. *Aerosol Science and Technology*, 46(5): 576–583, 2012. doi:10.1080/02786826.2011.648780.

[59] A. Mayer, A. Ulrich, J. Czerwinski, and J. Mooney. Metal-Oxide Particles in Combustion Engine Exhaust. *SAE Technical Paper 2010-01-0792*, 2010. doi:10.4271/2010-01-0792.

[60] K. McMahon, C. Selecman, F. Botzem, and B. Stablein. Lean GDI Technology Cost and Adoption Forecast: The Impact of Ultra-Low Sulfur Gasoline Standards. *SAE Technical Paper 2011–01–1226*, 2011. doi:10.4271/2011-01-1226.

[61] A. Miller, G. Ahlstrand, D. Kittelson, and M. Zachariah. The fate of metal (Fe) during diesel combustion: Morphology, chemistry, and formation pathways of nanoparticles. *Combustion and Flame*, 149(1-2):129–143, 2007. doi:10.1016/j.combustflame.2006.12.005.

[62] S. Mosbach, M. S. Celnik, A. Raj, M. Kraft, H. R. Zhang, S. Kubo, and K. Kim. Towards a detailed soot model for internal combustion engines. *Combustion and Flame*, 156(6):1156–1165, 2009. doi:10.1016/j.combustflame.2009.01.003.

[63] A. Neer and U. O. Koylu. Effect of operating conditions on the size, morphology, and concentration of submicrometer particulates emitted from a diesel engine. *Combustion and Flame*, 146(1-2):142–154, 2006. doi:10.1016/j.combustflame.2006.04.003.

[64] D. J. Rader and P. H. McMurry. Application of the Tandem Differential Mobility Analyzer to Studies of Droplet Growth or Evaporation. *Journal of Aerosol Science*, 17(5):771–787, 1986. doi:10.1016/0021-8502(86)90031-5.

[65] W. F. Rogge, L. M. Hildemann, M. A. Mazurek, G. R. Cass, and B. R. T. Simoneit. Sources of fine organic aerosol. 2. Noncatalyst and catalyst-equipped automobiles and heavy-duty diesel trucks. *Environmental Science & Technology*, 27(4):636–651, 1993. doi:10.1021/es00041a007.

[66] T. Rönkkö, A. Virtanen, K. Vaaraslahti, J. Keskinen, L. Pirjola, and M. Lappi. Effect of dilution conditions and driving parameters on nucleation mode particles in diesel exhaust: Laboratory and on-road study. *Atmospheric Environment*, 40(16):2893–2901, 2006. doi:10.1016/j.atmosenv.2006.01.002.

[67] T. Rönkkö, A. Virtanen, J. Kannosto, J. Keskinen, M. Lappi, and L. Pirjola. Nucleation mode particles with a nonvolatile core in the exhaust of a heavy duty diesel vehicle. *Environmental science & technology*, 41(18):6384–9, 2007. doi:10.1021/es0705339.

[68] H. Sakurai, K. Park, P. H. McMurry, D. D. Zarling, D. B. Kittelson, and P. J. Ziemann. Size-Dependent Mixing Characteristics of Volatile and Nonvolatile Components in Diesel Exhaust Aerosols. *Environmental science & technology*, 37(24):5487–95, 2003. doi:10.1021/es034362t.

[69] H. Sakurai, H. J. Tobias, K. Park, D. Zarling, K. S. Docherty, D. B. Kittelson, P. H. McMurry, and P. J. Ziemann. On-line measurements of diesel nanoparticle composition and volatility. *Atmospheric Environment*, 37(9-10):1199–1210, 2003. doi:10.1016/S1352-2310(02)01017-8.

[70] M. Sander, R. I. A. Patterson, A. Braumann, A. Raj, and M. Kraft. Developing the PAH-PP soot particle model using process informatics and uncertainty propagation. *Proceedings of the Combustion Institute*, 33(1):675–683, 2011. doi:10.1016/j.proci.2010.06.156.

[71] R. L. Schalla and G. E. McDonald. Variation in Smoking Tendency Among Hydrocarbons of Low Molecular Weight. *Industrial & Engineering Chemistry*, 45(7): 1497–1500, 1953. doi:10.1021/ie50523a038.

[72] J. J. Schauer, M. J. Kleeman, G. R. Cass, and B. R. T. Simoneit. Measurement of Emissions from Air Pollution Sources. 2. C 1 through C 30 Organic Compounds from Medium Duty Diesel Trucks. *Environmental Science & Technology*, 33(10): 1578–1587, 1999. doi:10.1021/es980081n.

[73] J. J. Schauer, C. G. Christensen, D. B. Kittelson, J. P. Johnson, and W. F. Watts. Impact of Ambient Temperatures and Driving Conditions on the Chemical Composition of Particulate Matter Emissions from Non-Smoking Gasoline-Powered Motor Vehicles. *Aerosol Science and Technology*, 42(3):210–223, 2008. doi:10.1080/02786820801958742.

[74] H. Seong, K. Lee, and S. Choi. Effects of Engine Operating Parameters on Morphology of Particulates from a Gasoline Direct Injection (GDI) Engine. *SAE Technical Paper 2013-01-2574*, 2013. doi:10.4271/2013-01-2574.

[75] A. J. Smallbone, A. R. Coble, A. N. Bhave, S. Mosbach, M. Kraft, N. Morgan, and G. Kalghatgi. Simulating PM Emissions and Combustion Stability in Gasoline/Diesel Fuelled Engines. *SAE Technical Paper 2011-01-1184*, 2011. doi:10.4271/2011-01-1184.

[76] srm suite user manual v6.1. *cmcl innovations*, 2009.

[77] S. E. Stein and A. Fahr. High-temperature stabilities of hydrocarbons. *The Journal of Physical Chemistry*, 89(17):3714–3725, 1985. doi:10.1021/j100263a027.

[78] V. Stone and K. Donaldson. Small particles - Big Problem. *The Aerosol Society: Newsletter*, 33, 1998.

[79] J. Storey, T. Barone, J. Thomas, and S. Huff. Exhaust Particle Characterization for Lean and Stoichiometric DI Vehicles Operating on Ethanol-Gasoline Blends. *SAE Technical Paper 2012-01-0437*, 2012. doi:10.4271/2012-01-0437.

[80] J. M. E. Storey, C. S. Sluder, D. A. Blom, and E. Higinbotham. Particulate Emissions from a Pre-Emissions Control Era Spark-Ignition Vehicle: A Historical Benchmark. *SAE Technical Paper 2000-01-2213*, 2000. doi:10.4271/2000-01-2213.

[81] J. Swanson and D. Kittelson. Evaluation of thermal denuder and catalytic stripper methods for solid particle measurements. *Journal of Aerosol Science*, 41(12):1113–1122, 2010. doi:10.1016/j.jaerosci.2010.09.003.

[82] H. J. Tobias, D. E. Beving, P. J. Ziemann, H. Sakurai, M. Zuk, P. H. McMurry, D. Zarling, R. Waytulonis, and D. B. Kittelson. Chemical analysis of diesel engine nanoparticles using a nano-DMA/thermal desorption particle beam mass spectrometer. *Environmental science & technology*, 35(11):2233–43, June 2001. doi:10.1021/es0016654.

[83] T. S. Totton, D. Chakrabarti, A. J. Misquitta, M. Sander, D. J. Wales, and M. Kraft. Modelling the internal structure of nascent soot particles. *Combustion and Flame*, 157(5):909–914, 2010. doi:10.1016/j.combustflame.2009.11.013.

[84] A. Violi, A. Kubota, T. N. Truong, W. J. Pitz, C. K. Westbrook, and A. F. Sarofim. A Fully Integrated Kinetic Monte Carlo/Molecular Dynamics Approach for the Simulation of Soot Precursor Growth. *Proceedings of the Combustion Institute*, 29(2): 2343–2349, 2002. doi:10.1016/S1540-7489(02)80285-1.

[85] E. Vouitsis, L. Ntziachristos, and Z. Samaras. Modelling of diesel exhaust aerosol during laboratory sampling. *Atmospheric Environment*, 39(7):1335–1345, 2005. doi:10.1016/j.atmosenv.2004.11.011.

[86] H. Wang. Formation of nascent soot and other condensed-phase materials in flames. *Proceedings of the Combustion Institute*, 33(1):41–67, 2011. doi:10.1016/j.proci.2010.09.009.

[87] K. T. Whitby and B. K. Cantrell. Atmospheric aerosols: Characteristics and measurement. In *Proceedings of the International Conference on Environmental Sensing and Assessment (ICESA), Institute of Electrical and Electronic Engineers (IEEE). IEEE #75-CH 1004-1, ICESA paper 29-1 (6pp). Washington, DC: IEEE*, 1976.

[88] A. Wiedensohler, H. C. Hansson, P. B. Keady, and R. Caldow. Experimental verification of the particle detection efficiency of TSI 3025 UCPC. *Journal of Aerosol Science*, 21:S617–S620, 1990. doi:10.1016/0021-8502(90)90318-R.

[89] J. Yi, S. Wooldridge, G. Coulson, J. Hilditch, C. O. Iyer, P. Moilanen, G. Papqaioannou, D. Reiche, M. Shelby, B. VanderWege, C. Weaver, Z. Xu, G. Davis, B. Hinds, and A. Schamel. Development and Optimization of the Ford 3.5L V6 EcoBoost Combustion System. *SAE International Journal of Engines*, 2(1):1388–1407, 2009. doi:10.4271/2009-01-1494.

[90] S. Zhang and W. McMahon. Particulate Emissions for LEV II Light-Duty Gasoline Direct Injection Vehicles. *SAE International Journal of Fuels and Lubricants*, 5(2): 637–646, 2012. doi:10.4271/2012-01-0442.

[91] P. J. Ziemann, H. Sakurai, and P. H. McMurry. Chemical Analysis of Diesel Nanoparticles Using a Nano-DMA/Thermal Desorption Particle Beam Mass Spectrometer, Final Report, CRC Project No. E-43-4, accessed January 19, 2014. 2002. URL http://www.crcao.com/.